ECONOMIC POLICY

73rd Economic Policy Panel Meeting

15-16 April 2021

The Role of Schools in Transmission of the SARS-CoV-2 Virus:
Quasi-Experimental Evidence from Germany

Kirill Borusyak (University College London)
Clara von Bismarck-Osten (University College London)
Uta Schoenberg (University College London)

CEPR   CESifo   SciencesPo.

The Role of Schools in Transmission of the SARS-CoV-2 Virus: Quasi-Experimental Evidence from Germany[1]

Clara von Bismarck-Osten[*], Kirill Borusyak[*†], and Uta Schönberg[*‡]

[*] University College London; [†] CEPR; [‡] IAB, RWI, and CReAM

March 19, 2021

Abstract

This paper considers the role of school closures in the spread of the SARS-CoV-2 virus. To isolate the impact of the closures from other containment measures and identify a causal effect, we exploit variation in the start and end dates of the summer and fall school holidays across the 16 federal states in Germany using a difference-in-differences design with staggered adoption. We show that neither the summer closures nor the closures in the fall had a significant containing effect on the spread of SARS-CoV-2 among children or a spill-over effect on older generations. There is also no evidence that the return to school at full capacity after the summer holidays increased infections among children or adults. Instead, we find that the number of children infected increased during the last weeks of the summer holiday and decreased in the first weeks after schools reopened, a pattern we attribute to travel returnees.

Keywords: Covid Economics, School Closures, Public Health

JEL codes: I10, I18, I28

1   Introduction

The coronavirus pandemic has sparked an international debate on the efficiency of school closures as a containment measure. Despite a "second wave" of infections by the SARS-CoV-2 virus (causing the "COVID-19" disease) starting in the early fall of 2020 and a surge in the representation of children among new cases after the start of the new academic school year (The New York Times, 2020; The Guardian, 2020; Die ZEIT, 2020), most European countries have kept their schools open throughout the fall. However, as infections rose sharply (as in the U.K.) or remained at stubbornly high levels (as in Germany) over the course of winter, many countries reconsidered the alleged "measure of last resort": the closing of schools. With the mounting concerns about the new strains of the virus, several European countries, including the United Kingdom and Germany, did not reopen schools after the end of the winter holiday – adding to the pressure to understand their role in the transmission of the SARS-CoV-2 virus.

Because of their widespread consequences, school closures are among the most controversial containment policies. Prolonged school closures may have a negative effect on the psychological and emotional development of children, and unequal remedial measures have been found to widen learning inequalities (Engzell et al., 2020; Andrew et al., 2020). School closures also negatively impact the careers of parents obliged to take on more educational responsibilities and reduce the number of hours supplied in the labor market (Fuchs-Schündeln et al., 2020). Since women typically shoulder most of the childcare responsibilities, it is also feared that school closures will widen the gender wage gap in the long run (Alon et al., 2020).

These costs are weighed against the effectiveness of school closures as a strategy to contain the spread of SARS-CoV-2. The main mechanism through which school closures are expected to be effective is by preventing social interactions among children in schools. Reduced contact between children may further break the chain of infection from child to parent and grandparent, thereby reducing infection rates in the adult population. School closures may also induce a series of either offsetting or reinforcing behavioural adjustments. On the one hand, children may substitute school interactions with other activities that introduce additional risks of transmission. On the other hand, school closures could force parents to work from home, reducing their work-related contacts and, thereby, their risk of contagion.[2]

We aim to identify the effect of school closures on children as well as various age groups of adults. Understanding the "spill-over" effects on adults is of central importance, as the severity of the

---

[2] A more worrying labour force response would constitute in the reduction of the health-care workforce available. A study in the United States estimates that a total of 28.8% of healthcare providers have childcare obligations (Bayham and Fenichel, 2020).

disease has been found to be closely linked to age. Adults are relatively overrepresented among confirmed COVID-19 cases and have a higher risk of dying from the disease, with 94% of the deaths in Germany attributed to the group aged 60 and above. Children under the age of 15, by contrast, account for only 9.6% of cumulative confirmed SARS-CoV-2 cases, despite making up 13.6% of the country's population.[3] They almost always experience mild symptoms (Wang et al., 2020), although recent reports suggest a small increase in the incidence of children experiencing severe inflammatory symptoms, which could be linked to SARS-CoV-2 (Pouletty et al., 2020).

In this paper, we consider school closures and openings as "treatments" and apply modern econometric tools to identify the "causal" effects of school closures and reopenings on SARS-CoV-2 infections among children, as well as their potential spill-over effects on adults. We exploit variation in the start and end dates of school summer and fall school holidays across the federal states ("Bundesländer") of Germany for difference-in-differences identification, building on the strategy developed by Adda (2016) in the context of influenza, gastro-enteritis, and chickenpox in France. The sixteen states of Germany have staggered summer holidays to avoid overcrowding the national travel infrastructure. In 2020, children in the state of Mecklenburg-Western Pomerania began their summer holiday on June 20, whereas children in Baden Wurttemberg had to wait a further six weeks, until July 30. Similarly, the fall holidays, which are typically two weeks long, started on October 3 in the states of Schleswig-Holstein children and Hesse, but not until October 24 and 31 in the states of Baden Wurttemberg and Bavaria. We exploit this quasi-experimental variation using an estimator developed by Borusyak et al. (2021) for difference-in-differences settings with staggered adoption of treatment and heterogeneous treatment effects, which offers advantageous robustness and efficiency properties.

Two features of the German summer and fall holidays make them attractive as the source of causal identification. First, whether the holiday starts early or late in each state is decided upon years in advance and was unaltered by the pandemic. Therefore, the variation in the start and end date of the holidays across German states was not confounded by the spread of SARS-CoV-2 within the state. Second, in contrast to school closures during the first lockdown in March, the start and end of the summer school holidays did not coincide with the introduction of other containment measures, such as the closing of bars, restaurants and non-essential shops, allowing us to isolate the impact of school closures. This was also the case for the fall holidays, with the exception of a partial lockdown announced at the federal level implemented November 2, which is why we focus on the fall holiday

---

[3] These estimates were computed on our own, based on the data described in Section 2.3 and covering June 1 through October 28, 2020.

closures (but not subsequent reopening) and restrict the empirical analysis to the period preceding the lockdown announcement, October 28.[4]

Difference-in-differences estimation of the effects of school closures and reopenings on the incidence of SARS-CoV-2 at the regional level is also attractive from a policy perspective. These estimates identify an overall impact, encompassing all the behavioural adjustments that school closures bring about, such as increased activities of children outside school and the reduced work-related contacts of parents. Moreover, the baseline against which school closures are evaluated is not the status quo before the pandemic, but a situation in which various other containment measures are in place. By analysing the effects of both school closures and reopenings, we evaluate whether schools that operated at partial capacity (as it was the case before the summer holidays) play a more limited role in spreading SARS-CoV-2 than schools that reopened to full capacity, with additional hygiene rules and other restrictions, at the end of the summer holidays. By comparing the effects of the summer and fall holiday closures, we assess whether closures are more effective at containing the spread of SARS-CoV-2 in situations when cases in the population are high (as in the fall) compared to situations when they are low (as in the summer). A heterogeneity analysis that compares the effects of summer reopenings in districts with below and above median infection rates provides additional insights into the same question. Our estimates are, therefore, directly informative on the trade-offs that policymakers may face in the future – an important advantage of our design over those pursued by some existing studies (summarized in Section 2.1).

At the same time, some limitations of our methodology are worth pointing out. The summer holidays are a time of increased travel for families. Most likely, this increased the risk of infection, either because infection rates in typical destination regions were higher than in Germany or because travelling itself poses a risk. With our strategy, it is challenging to disentangle any rise in confirmed COVID-19 cases due to travel from a rise due to school reopenings *per se*. To tackle this difficulty, we leverage the exact timing of the increases in cases around the date of school reopening after the summer holidays and draw on state-level data on the share of confirmed positive cases to determine the most likely explanation. Our analysis of the fall holidays is less likely to be contaminated by travel behavior since families travel considerably less during the fall than the summer. Yet, this analysis is limited by the short duration of the fall holidays and sparser cross-state variation in their timing, preventing us from considering fall school closures and reopenings as separate events.

We find little evidence that school closures in the summer lowered SARS-CoV-2 infection

---

[4] The lockdown implemented on November 2 involved closures of cultural entertainment venues, restaurants, pubs and bars. Schools and day care centers were set to remain open. By October 28, the fall holidays have ended in most states with the exceptions of Thuringia, Saxony, Baden Wuerttemberg, and Bavaria.

rates among school-aged children or elder generations. At best, according to the lower bound of the 95% confidence interval of our baseline estimates, only 0.335 infections per 100,000 school-aged children (ages 5-14) and 0.026 infections per 100,000 adults aged 60 and above have been prevented per day in the first three weeks of the school summer holidays.

Similarly, we do not find that the return to full-time schooling after the summer break led to an increase in infections among school-aged children. Instead, we find that SARS-CoV-2 infection rates tend to increase in the last weeks of the summer holidays and to decline in the first days after schools open, a pattern visible in all age groups, but more pronounced in the younger population. We consider this to be best explained by a higher risk of infection of families returning home from their travels shortly before the summer holidays ended and increased testing of them.[5]

Our analysis of the fall holidays confirms that school closures did not significantly reduce COVID-19 cases among either children or adults, even in situations of higher incidence levels. These results are, however, limited to two weeks after the holiday began and may therefore not capture spillover effects that take longer to appear. They are also less precisely estimated.

In sum, our findings suggest that schools have played a limited role in the transmission of SARS-CoV-2 over the summer and fall of 2020. Importantly, our results provide little support for the hypothesis that school openings at the start of the academic year substantially contributed to the second wave of infections, or to the surge in the representation of children among new cases. We acknowledge that both the summer and fall holidays in Germany precede the spread of new variants of SARS-CoV-2, most importantly the "British" B.1.1.7, the "South-African" 501Y.V2, and the "Brazilian" P.1 and P.2 strains, that may be more infectious or more resistant to available vaccines than the previous strains. Our findings based on the summer and fall holidays may therefore understate the containing effect of school closures in countries where such variants are widespread. On the other hand, as the share of vaccinated adults in the population grows, the spillover effects on infection rates of adults and, in particular, deaths may also be smaller than those we uncover.

The remainder of this paper is organised as follows. Section 2 summarizes related literature, provides background information on the containment measures implemented, the scheduling of the school holidays as well as the spread of the SARS-CoV-2 virus in Germany, and introduces the data. The empirical strategy is described in Section 3. Section 4 reports the empirical results, and Section 5 concludes.

---

[5] This explanation is supported by the finding of Isphording et al. (2020) that incoming mobility, but not outcoming mobility, increased during the last two weeks of the summer holidays in Germany.

2 Background

2.1 Related Literature

The effectiveness of school closures as an important "non-pharmaceutical intervention"[6] has been studied by a wide range of disciplines, including epidemiology, virology, paediatrics, psychology, and economics, with mixed empirical findings.

Most papers can be attributed to the category of correlational studies, studying the relationship between in-person schooling and the incidence of COVID-19 across counties or states within a country (e.g., Auger et al., 2020, Goldhaber et al., 2021 and Harris et al. 20201 for the US and Dehning et al., 2020 for Germany) or across countries (Liu et al., 2021). These studies have reached conflicting conclusions, ranging from no measurable impact of in-person schooling on infection rates (e.g., Harris et al., 2021) to important containing effects (e.g., Liu et al., 2021).[7] One important drawback of these correlational studies is that schools often open or close in response to rising or declining infections in the local area or country, impeding a causal interpretation. A second drawback is that in some studied cases (e.g., Dehning et al., 2020) school closures were enforced at the same time as other lockdown measures, making it impossible to isolate the impact of school closures from the impact of these alternative containment measures.

Quasi-experimental studies, such as ours, overcome both drawbacks. School holidays offer an interesting source of quasi-experimental variation. Adda (2016) first leveraged them to study the transmission of viral diseases such as gastro-enteritis and influenza among both children and adults and found schools to be successful at curbing the spread of these viral diseases.[8] However, the paper closest to ours is the contemporaneous work by Isphording et al. (2020), in which a similar research design was used to estimate the impact of school reopenings after the end of the German summer holiday. While our results are broadly in line with theirs, two differences are worth noting. Their analysis exclusively focuses on the reopening of schools at the end of the summer holiday, while we evaluate school closures and reopenings in the summer as separate events and provide complementary evidence on the closures induced by the fall holiday. In addition, we pay extra attention to the period

---

[6] Epidemiological term for containment measures which do not involve medication or vaccination. For the economics literature on other non-pharmaceutical interventions see, for example, Fetzer (2020) and Mangrum and Niekamp (forthcoming) who study the effects of keeping restaurants and universities open, respectively.

[7] In one of the analyses, Harris et al. (2021) also leverage variation in teacher bargaining power across counties in the U.S., which is correlated with whether or not schools in the county operate in person, to obtain causal effects. This quasi-experimental approach is closer to the small literature we describe next.

[8] One explanation for the difference in Adda's and our findings could lie in the differences between SARS-CoV-2 and other viruses. Alternatively, the difference could stem from the hygiene rules and procedures currently in place in schools to avoid contagion, which are not typically implemented during the seasonal outbreaks of other diseases studied by Adda (2016).

just before schools reopened in the summer and identify a significant temporary increase in infection rates during that time. This leads us to conclude that travel returnees exposed to a higher risk of infection may have contributed to the spread of SARS-CoV-2. Another relevant quasi-experimental study on the question of the role of schools in the spread of COVID-19 is the paper by Vlachos et al. (2021). The "experiment" exploited is that lower secondary schools in Sweden remained open, whereas upper secondary schools moved online. While they found a greater risk for in-person teachers of contracting the virus, the spillover effects to the general population were small, leaving the authors to conclude that schools play a minor role in the spread of the SARS-CoV-2 virus.

A separate and complementary strand of studies conducted by epidemiologists and virologists informs about the effectiveness of school closures in a more indirect way: by analysing infection rates among children and, in turn, their own infectiousness. One common approach is to study infection rates and antibody prevalence in a single school or a set of schools where infections have been reported.[9] Such studies, commonly referred to as "cohort" studies, have reached different conclusions on plausible infection rates among children. Fontanet et al. (2020) found a high infection rate among pupils in an early outbreak in a French high school, while more recent larger-scale studies generally reported smaller infection rates (Berner 2020; Ulyte et al. 2020; Ladhani et al. 2021).[10] Contact tracing studies go a step further, analysing the extent to which infected children spread the virus to members of their immediate network, such as their parents and siblings. While a small-scale study for Trento, Italy found that children under 15 years were the most contagious of any age group (Fateh-Moghadam et al. 2020, with a sample size of 14), two larger-scale studies for South Korea and Australia did not find schools to be risky when infection rates are low (Yoon et al., 2021; Macartney et al., 2020). An alternative approach to evaluate the infectiousness of children is taken in studies that compare the viral load in the upper respiratory tract in test samples of infected children and adults. Most such studies published in the summer 2020 found no evidence of a smaller viral load in children than in infected adults (e.g., Jones et al., 2020; Heald-Sargent et al., 2020) and concluded that children may be as infectious as adults.

Cohort, contact tracing and viral concentration studies often come with a host of caveats, including small and not representative samples; neither do these studies provide direct evidence on the role of schools in the transmission of SARS-CoV-2. An important advantage of our approach is that we provide direct estimates of the effects of school closures, drawing on data comprising all

---

[9] Typically, those estimates subsequently feed into models that project the spread of the virus in the general population.
[10] Berner et al. (2020) survey schools in and around Dresden, Germany. Ulyte et al. (2020) study seroprevalence in 55 randomly selected schools in the canton of Zürich, Switzerland. Finally, Ladhani et al. (2021) test children across 131 schools in England.

infections in a country. Our estimates are policy relevant as they capture the overall impact, encompassing all behavioural adjustments that school closures bring about, and take into account the current situation under which schools operate.

2.2 The Institutional Setting in Germany

Germany's Policy Response to the Pandemic

Drawing on the experience with influenza where school closures proved particularly effective (Viner et al., 2020; Adda 2016), all German states proceeded to closing schools early in the outbreak of SARS-CoV-2, around March 16, 2020. Around the same time, other containment measures such as the closing of bars, restaurants, and non-essential shops, as well as social distancing rules were implemented, and these measures were often timed similarly across states (see the see IAB database on the containment measures in Germany[11]; Bauer and Weber, 2020). Schools gradually reopened after the Easter holidays (around April 27), prioritising the cohorts having examinations. This reopening similarly tended to coincide with lifting other containment measures (Federal Government of Germany, 2020). This policy environment makes the spring period unsuitable for our analysis: the variation in the timing of school closures is limited, and it appears difficult to disentangle the various containment measures.

In the first period of our interest – from the June 1 to the respective start of the summer holidays – the focus was placed on ensuring social distancing of 1.5m between children and teachers both in the classroom and buildings; shifts were also introduced in many schools (Frankfurter Allgemeine Zeitung, 2020). This was accompanied by a set of policies introduced similarly across states: ventilation in schools at regular intervals, hygiene standards, and the exclusion from lessons if a student develops symptoms (Tagesschau, 2020b). On the other hand, it was the task of every school to gauge how best to guarantee compliance with social distancing rules and government guidelines. Moreover, the handling of outbreaks in school and the quarantine enforcements were (and still are) in the authority of the 375 local health authorities, and nothing suggests systematic variation across states in that regard.

After the last states entered school holiday, the Federal Government introduced new policies concerning the testing of travel returnees. On August 1, the federal government waived the cost of testing for these returning travellers, and on August 8, it introduced compulsory testing for travellers

---

[11]The database can be found under the following link: https://iab.de/de/daten/corona-eindaemmungsmassnahmen.aspx.

returning from high-risk countries. These policies were enforced nationwide, and *during* the school holiday of most states (with the exception of Mecklenburg Western Pomerania).[12]

Upon the start of the new academic year, the state governments and ministers of educations coordinated to ensure schools across Germany would return to teaching at full capacity (Handelsblatt, 2020). As the 1.5m social distancing rule was impossible to impose with schools fully open, all states advised that schools should set "contact groups" (usually classes or cohorts) within which mixing is allowed. Most states refrained from making masks compulsory in classrooms (with two temporary exceptions: Bavaria and North-Rhine-Westphalia for the first two to three weeks after holiday; see Bayerischer Rundfunk, 2020 and ZDF Heute, 2020a). Guidelines regarding ventilation, hygiene standards, and exclusion from lessons if a student develops symptoms remained in place while local health authorities continued to be responsible for the handling of confirmed cases.

In the fall, as cases started to increase, some additional measures were implemented. Most importantly, Germany announced on October 28 and implemented on November 2 a partial nation-wide lockdown, involving closures of for example entertainment venues and restaurants. Schools and day care centres, however, were set to remain open. This partial lockdown does not affect our analysis on the closures and reopenings in the summer but overlaps with the fall holiday in Bavaria (and marginally in three other states where the holiday ended on November 2). When analysing the impact of fall holiday closures on COVID-19 cases, we therefore restrict our analysis to infections up to October 28, the day the lockdown was announced. Another reason to discard this period is that the return to school after the fall holidays coincided with several states making masks mandatory.[13]

To summarize, the summer holiday school closures happened in an environment where schools are only partially open, social distancing is encouraged, and guidelines regarding ventilation, hygiene standards and how to handle confirmed cases are in place. In contrast, summer holiday school reopenings and fall holiday school closures correspond to a situation where schools operate under full capacity, social distancing within classrooms is impossible, masks are not compulsory but plans regarding ventilation, hygiene standards and handling of confirmed cases are in place.

The Summer and Fall School Holidays

Since our empirical strategy will exploit the variation in the start and end dates of the summer and fall holiday across the 16 German states, it is important to explain the process

---

[12] In Mecklenburg-Western Pomerania the summer holidays ended on August 2, and tests were made compulsory at the state level beforehand (Deutschlandfunk, 2020).
[13] These states are: Baden-Württemberg, North Rhine-Westphalia, Schleswig Holstein, Brandenburg, Bremen and Hamburg (ZDF heute, 2020b).

generating this variation. In Germany, both summer and fall school holiday dates are planned several years in advance, with most states alternating between early and late summer holiday starting dates.

Figure 1 offers an overview of the holiday start and end dates in the summer (Panel A) and fall (Panel B) of 2020. Summer holidays last six weeks in all German states. There are also six weeks between the states with the earliest and latest start of the school summer holidays. The summer holiday period stretches across almost three months, with the first schools closing on June 20 and last schools reopening on September 13 (where we define holidays as including the surrounding weekends). The fall holiday starts as early as October 3 in the states of Mecklenburg Western Pomerania, Schleswig-Holstein, Hesse, and Hamburg and as late as October 24 and 31 in the states of Baden Wurttemberg and Bavaria. In 12 out of the 16 states, fall holidays last two weeks; in four states, they last one week only.

Figure 2 illustrates the geographic variation in the summer holiday start date, showing that summer school holidays started first in one of Germany's most Northern states (Mecklenburg Western Pomerania) and last in Germany's most Southern states (Baden Wurttemberg and Bavaria). The predetermined order in which states enter the fall holiday is generally similar to that in the summer (see Panel B of Figure 1).

2.3 Data

We obtain the key data on infections from the Robert Koch Institute (RKI), a federal government agency responsible for the prevention and control of epidemics in Germany, as well as for epidemiological research. Their database has recorded all confirmed positive cases in Germany on a daily basis since the first COVID-19 case was reported on January 15, 2020.[14] In our empirical analysis, we use data up until October 28, 2020. The data are available at the county ("Landkreis" or "Stadtkreis") level. Berlin constitutes an exception, where the data are available by borough ("Bezirk"). Altogether, the dataset comprises 415 regional entities which we refer to as districts.

We process the original case-level data to construct a daily panel of regions. The time dimension is given by the "reporting date": the date when a case became known to the local health department, which is generally the same day the test results were received.[15] The regional

---

[14] Retrieved on March 14, 2020 from:
https://www.arcgis.com/home/item.html?id=f10774f1c63e40168479a1feb6c7ca74.
[15] Source: RKI, phone interview. For around 60% of cases a "reference" date is also provided, when the first symptoms appear. However, due to a large fraction of missing data (in particular, because of asymptomatic cases), we do not use

dimension corresponds to the district in which the positive case is registered, i.e., in which the person is staying on the reporting date and where the quarantine regulation is enforced. While this district may not always correspond to the place of residence, it is to be expected that the wide majority get tested in their place of residence.[16]

Each case is classified into age brackets of 0–4, 5–14, 15–34, 35–59, 60–79 and over 80-years-old. We will consider the 5–14 group that roughly corresponds to children in primary and lower secondary school, two groups of adults (with the 15–34 group including high school and college students), and a combined group of seniors, i.e. 60 years and older. Cases are further classified into either recovered or deceased, allowing us to count deaths.[17] We note that the deaths are coded according to the reporting date – the day on which the deceased person tested positive for the virus – and not the day of death.

We then normalize the cases by the age-bracket specific regional population (in 100,000 people) before the pandemic, retrieved from the regional database ("Regionaldatenbank") and corresponding to December 31, 2018.[18] For the boroughs of Berlin, the data were instead obtained from the Statistical Office of Brandenburg-Berlin as of December 31, 2019.[19]

We note that confirmed cases as reported by the RKI may understate the true infection rates as some asymptomatic cases may remain undetected. This may lead to an underrepresentation of children who are more frequently asymptomatic (Robert-Koch Institut, 2020) among confirmed cases. However, it is to be expected that confirmed cases capture nearly all cases that led to serious disease. Moreover, we are not aware of any reasons for why the underrepresentation of asymptomatic children should systematically vary across districts or states. Thus, our estimates for the effects of school closures and openings on infection rates of children may be somewhat attenuated but not otherwise biased.

For our robustness checks and heterogeneity analyses, we further leverage additional data sources. We use a database on the number of administered positive polymerase chain reaction (PCR) tests and the fraction of positive tests by state and date (but not age) based on a sample of

---

these reference dates in the analysis.

[16] That is because the states in Germany typically advise for (or require) testing *upon return* from travels, as well as *before* travels at the place of residence (Tagesschau, 2020a).

[17] Cases which are still ongoing are classified as neither recovered nor deceased. Since our analysis is restricted to reported dates up to October 28, the censoring problem from such cases is negligible.

[18] Retrieved on August 7, 2020 from:
https://www.regionalstatistik.de/genesis/online?language=de&sequenz=tabelleAufbau&selectionname=12411-04-02-4#astructure.

[19] Retrieved on October 12, 2020 from: https://www.statistik-berlin-brandenburg.de/datenbank/inhalt-datenbank.asp.

laboratories across Germany, voluntarily reporting to the RKI.[20] These data capture 35.7% of all confirmed cases between June 1 and October 28, 2020. We approximate the total number of administered PCT tests (including laboratories that are not participating) as the ratio of the total number of cases from our main data to the share of positive tests.

We also construct several control variables. We retrieve data on average daily temperature from 580 weather stations.[21] For each district and day, we then average the temperature reported by the five stations closest to the district centroid, placing a higher weight on the closest ones.[22] Furthermore, we measure district-specific tourist intensity in two ways: (i) as the number of guest arrivals in accommodation facilities in 2019, as reported by the regional database ("Regionaldatenbank"),[23] and (ii) as the exposure to an international airport, measured as $20/(20 + distance)$, where $distance$ is the distance in kilometers between the district centroid and the closest international airport.[24] The coordinates of the district centroids are from the Federal Agency for Cartography and Geodesy[25] and the coordinates of the 22 international airports stem from Google Maps. Finally, we use population density by district for year 2019, as reported by the RKI.[26]

2.4 A Descriptive Outlook on the Spread of SARS-CoV-2 in Germany

Before proceeding to the analysis, we provide an overview of the dynamics of the SARS-CoV-2 spread in Germany. Figure 3 contrasts daily cases (Panel A) and daily deaths (Panel B) per 100,000 inhabitants in Germany, the United States, as well as four selected European countries (France, Italy, Sweden and the United Kingdom), based on the data from the European Centre for Disease Prevention and Control (ECDC).

In Germany, the peak of daily cases in the first wave of new infections was reached on the March 27, 2020, with 8.27 reported cases per 100,000 inhabitants (6,933 overall), and the peak of

---

[20] The data were provided to us by the RKI by request. The fraction of positive tests is rounded to two digits. Since 0.00 indicates "below 0.005," we replace such zeros with 0.0025.

[21] Retrieved on February 10, 2021 from:
https://opendata.dwd.de/climate_environment/CDC/observations_germany/climate/daily/kl/recent/.

[22] Specifically, the weights are proportional to 1/(1+distance in km).

[23] Retrieved on February 10, 2021 from:
https://www.regionalstatistik.de/genesis//online?operation=table&code=45412-03-02-
4&bypass=true&levelindex=0&levelid=1615732773390#abreadcrumb.

[24] We follow the German Airport Association's ("Flughafenverband ADV") definition of international airports in Germany.

[25] Retrieved on February 10, 2021 from: https://gdz.bkg.bund.de/index.php/default/digitale-geodaten/nicht-administrative-gebietseinheiten/gebietseinheiten-1-250-000-ge250.html.

[26] Retrieved on August 24, 2020 from: https://npgeo-corona-npgeo-de.hub.arcgis.com/datasets/917fc37a709542548cc3be077a786c17_0?geometry=-20.631%2C46.211%2C42.650%2C55.839.

daily deaths on April 15 with 0.61 deaths per 100,000 (510 overall).[27] Daily cases remained relatively low – fewer than one reported case per 100,000 – throughout May and June when lockdown measures were gradually eased. Since late-July, reported cases have been steadily increasing, with a noticeable uptick in cases in early October. For the first time on October 14, the ECDC reported more cases per 100,000 than at the peak of the first wave. Daily cases have remained high, around 20 per 100,000, throughout November, December and January and have declined moderately in February 2021.

By international comparison, Germany showed a similar trend in newly reported cases as other European countries such as Italy, France and the United Kingdom between March and June. While most European countries experienced an acceleration in daily reported cases during the fall, the increase and subsequent decline have been less pronounced in Germany than in France, the United Kingdom, and Italy. The United States followed a different time pattern, in that new cases per 100,000 never fell below 9 per day since April 2020 reached a first peak of about 20 in late July, and started increasing again in September, albeit at a slower pace than in most European countries.

Relative to other countries, Germany stands out in terms of the relatively low death toll during the first wave of the pandemic. At the peak of the first wave, the death rate per 100,000 inhabitants was about 0.61 in Germany, but above 1 in Italy, France, the United Kingdom and Sweden. Throughout fall and early winter, Germany experienced similar death rates per 100,000 as other countries. In Germany, and likewise for other countries, adults aged 60 and above have a considerably higher risk of dying from the COVID-19 disease. They make up 94% of all deaths in Germany in our study period.

Figure 4 shows daily SARS-CoV-2 cases per 100,000 over time by six age brackets for the period of our empirical analysis. Strikingly, during the first wave of the pandemic in March and April—when, for the most part, schools were closed due to general lockdown measures—infection rates among children (aged 14 and below) were low, both in absolute terms and relative to other age groups. In contrast, during the "second wave" of the pandemic in September and October—when schools were open—infection rates among children rose at a similar pace to those of adults, although infection rates continue to be lower among children than adults. The resulting increase in the share of children among newly confirmed cases appears to coincide with the end of the summer school holiday and has been linked to school openings by the press (The New York Times, 2020; Die ZEIT, 2020). The quasi-experimental variation in the school holiday dates in Germany offers a unique

---

[27] These numbers are based on the data from the European Centre for Disease Prevention and Control (ECDC). According to the RKI database (which our empirical analysis relies on), the peak of daily new cases and daily new deaths were both reached on the April 2, 2020, with 7.88 reported cases per 100,000 inhabitants (6,553 overall) and 0.50 deaths per 100,000 (415 overall). Note that the RKI database reports the date the deceased person was reported positive, and not the date of death.

setting to investigate that relationship in a rigorous manner.

3 Methodology

We build on Adda (2016) and exploit the variation in the timing of summer and fall school holidays across German states to isolate the impact of school closures and reopenings from other factors on the spread of SARS-CoV-2. As outlined in Section 2.2, the schedule of school holidays in 2020 was unaltered by the pandemic and did not coincide with other state-specific lockdown measures. The German setting is particularly interesting in this context, since the variation in the timing of both summer and, to a smaller extent, fall school holidays is larger than in other countries.

For identification, we rely on a difference-in-differences design with staggered adoption of treatment. This methodology assumes that the true causal model for the outcome of interest reported in district i on day t is

$$Y_{it} = \alpha_i + \beta_t + \tau_{it} D_{it} + \varepsilon_{it}. \tag{1}$$

Here α_i and β_t capture the district and day fixed effects and $D_{it} = 1[t \geq E_i]$ is the indicator that the district is "treated" (i.e., schools have closed or reopened, depending on the analysis), where E_i is the day when district i is treated. We separately consider three treatments: school closures and openings in the summer and the closures in the fall. Further, τ_{it} captures the "treatment effect"—that is, the impact of the school closures and openings on the spread of SARS-CoV-2—while ε_{it} is the residual such that $E[\varepsilon_{it} \mid \alpha_i, \beta_t, D_{it}] = 0$. The model in (1) incorporates the parallel trends assumption, whereby the expected outcome absent the treatment is $\alpha_i + \beta_t$. It also allows for heterogeneous treatment effects by district and time, and thus by the number of days since treatment.

To characterize treatment effects, we use the "imputation estimator" of Borusyak et al. (2021). A recent literature has shown that estimating equation (1) as a conventional event study, i.e. by Ordinary Least Squares (OLS) with two-way fixed effects and some lags and leads of treatment, produces estimates that are not reliable in presence of effect heterogeneity and potentially even have a wrong sign.[28] Several robust estimators have been recently proposed (e.g., de Chaisemartin and D'Haultfœuille, 2020; Sun and Abraham, forthcoming). Relative to these estimators, the imputation estimator possesses attractive efficiency properties, is transparent, and conservative standard errors are available for it, which can be computed analytically.[29]

---

[28] Borusyak and Jaravel (2017), de Chaisemartin and D'Haultfœuille (2020), Goodman-Bacon (2020), and Strezhnev (2018) establish this result in slightly different ways.

[29] We implement the analysis using the *did_imputation* Stata command provided by Borusyak et al. (2021).

The imputation estimator is constructed in three steps. First, the district and day fixed effects α_i and β_t in equation (1) are estimated by OLS on the subsample of untreated observations only, i.e. those with $D_{it} = 0$. In the case of the school closures we, therefore, estimate α_i and β_t using the data until the last day of school before the start of the holiday in each state. Second, we obtain an unbiased estimate $\hat{\tau}_{it} = Y_{it} - \hat{\alpha}_i - \hat{\beta}_t$ for each treated observation. While treatment effects for each day and district cannot be estimated consistently, Borusyak et al. (2021) show that averages of $\hat{\tau}_{it}$ across many observations can, under appropriate regularity conditions. Any such average of interest can therefore be reported in the third step. We focus here on the average effect a given number h days since treatment ($h \geq 0$):

$$\hat{\tau}_h = \frac{1}{|I_h|}\sum_{i\in I_h} \hat{\tau}_{i,E_i+h},$$ (2)

where I_h is the set of districts i observed in period $E_i + h$.

For each horizon h, the imputation estimator leverages all difference-in-differences contrasts between some district i in period $E_i + h$ (i.e., on a day h days after treatment) relative to periods before treatment, $t < E_i$ (reference periods), and relative to other districts which have not been treated yet by $E_i + h$. This estimator is only available for $h < H$, where H is the gap between the earliest and latest event dates observed in the sample (six weeks in our case for summer holidays, or five weeks with a reasonable sample size). This is in contrast to OLS estimates which are in principle possible to estimate for any long horizons but may not be reliable: there are no difference-in-differences contrasts that can directly identify those effects, and the estimates are obtained solely by extrapolations appropriate only under constant treatment effects. We focus on the effects of the school closures and openings in the summer up to three weeks after the beginning and end of the summer holiday (i.e., for $h = 0, ... ,20$).

In our baseline specification, we define the outcome variable Y_{it} as the number of confirmed COVID-19 cases per 100,000 inhabitants in some age bracket. We distinguish between children aged from 5 to 14 years old, whose infection risks may be directly reduced by school closures, and adults, for whom the effects are indirect. Limited by our data, we consider three adult age groups: a group of young adults between 15 and 34 years old; a group of middle-aged adults between 35 and 59 years old, in which most parents of school-aged children will fall; and a group of vulnerable adults older than 60 years of age. We also consider the number deaths per 100,000 inhabitants in the 60+ age group only, since 94% of the deaths are concentrated in that group.

We start out by estimating the effects of the school closures in the summer on the spread of SARS-CoV-2. To provide empirical support for the assumption of parallel trends, we follow Borusyak et al. (2021) and estimate the regression on the set of untreated observations only:

$$Y_{it} = \alpha_i + \beta_t + \sum_{p=-P}^{-1} \gamma_p 1[t = E_i + p] + \varepsilon_{it}. \tag{3}$$

Here, $1[t = E_i + p]$ are indicator variables of being treated 1 to P days later; we set $P = 14$. The comparison group here includes all observations for which treatment happens more than P days later. A conventional joint test of $\gamma_p = 0$ is then performed, and the magnitude of $\hat{\gamma}_p$ can be visually examined. It is important to note that this approach for pre-trend testing differs from the convention where pre-trend or placebo coefficients are estimated jointly with the treatment effects $\hat{\tau}_h$. Borusyak et al. (2021) explain three advantages of this approach. First, it clearly separates validation of the design (i.e., of the ex-ante assumption of parallel trends) from estimation given the design. Second, by imposing no pre-trends at the estimation stage, it improves efficiency of treatment effect estimation: all untreated observations are used in the imputation. Third, it removes the correlation between the treatment effect and the pre-trend estimators; such correlation introduces bias when the researcher follows the conventional practice of trusting the results only conditionally on the pre-trend test passing (Roth, 2020).

When turning to the effects of school reopenings in the summer, we additionally allow for "anticipatory" effects of treatment present up to K days before treatment; we set $K = 14$. We do this to allow for the possibility that SARS-CoV-2 infection rates may increase prior to school openings due to travel returnees and increased testing. Families often return home in the last two weeks of the summer holiday and typically spend their vacation in regions where infection rates were higher than in Germany and were tested upon returning home. The imputation estimator extends directly to the case of anticipation effects, with the treatment indicator redefined to switch to one K days before treatment: $D_{it} = 1[t \geq E_i - K]$. We (re)estimate district and day fixed effects α_i and β_t in equation (1) using only those observations that are assumed to be unaffected by the school opening treatment (i.e., observations more than two weeks before the end of the summer school holiday). We also check for "pre-trends" in a similar way as for school closures, by estimating equation (3) on a set of untreated observations and by testing whether the γ_p coefficients are individually and jointly equal to zero.

It should be noted that when examining the effects of school reopenings on the spread of SARS-CoV-2, we implicitly assume that the preceding school closures in the summer have had no impact on SARS-CoV-2 infection rates. We explicitly investigate and provide empirical support for this assumption in the first part of the empirical analysis, where we study the effects of summer school closures on the spread of SARS-CoV-2.

15

In the final step of the empirical analysis, we estimate the effects of fall holiday closures on the spread of SARS-CoV-2. We consider anticipatory effects due to travelling behavior unlikely in this context and therefore test for differential pre-trends in the 14 days prior to the start of the school holiday (i.e., we set $K = 0$ and $P = 14$). As Panel B of Figure 1 shows, the difference in the start dates of the fall holidays between states that introduced them first and last is four weeks (compared to six weeks for the summer holidays), so that we could in principle estimate the effects of fall school closures up to four weeks since the start of the fall holiday. However, the state in which fall holidays started latest (Bavaria) appears to exhibit a different time trend in infection rates from other states and thus is not a reliable control group. Hence, estimates for the impact of fall school closures on the spread of SARS-CoV-2 beyond the first two weeks rest on a single state (Baden Wuerttemberg). We therefore focus on effects in the first two weeks after the start of the fall holiday and do not consider fall school closures and reopenings as separate events.

We probe the robustness of our results to alternative estimation methods including a conventional event study and the de Chaisemartin and D'Haultfœuille (2020) estimator, and to the inclusion of additional control variables in Section 4.4. We report standard errors clustered at the level of NUTS-2 regions ("Regierungsbezirke," 38 clusters) throughout the paper. Standard errors clustered at the level of 16 states turn out to be *smaller* than standard errors clustered at the NUTS-2 level, prompting us to display the more conservative standard errors instead.

4   Empirical Findings and Discussion

4.1 The Effect of Summer School Closures on the Spread of SARS-CoV-2

The Impact of School Closures on Infection Rates among Children

We begin by examining the impact of the school closures induced by the summer holidays on infection rates among school-aged children. In Panel A of Figure 5, we group states into six cohorts according to their school summer holiday start date, ranging from June 20 (thick black line) to July 30 (thin green line), and display COVID-19 cases per 100,000 children, smoothed using a moving average filter with three lags and three leads, from June 1 until schools reopen at the end of the holiday. The vertical lines indicate the respective starts of the summer holiday. The infection rates among children do not show systematic variation in the three weeks leading up to the summer holiday, as well as the first three weeks of holiday.[30] Panel A therefore already provides little descriptive

---

[30] We acknowledge that the trajectories of infections are not literally parallel across cohorts, which may simply reflect random noise or may be due to differential (persistent or transitory) trends. By using clustered standard errors, we take into account the uncertainty in the estimates driven by such trends. In Section 4.4 we further show robustness to deviations from parallel trends, such as allowing for controls that enter the no-treatment potential outcome.

evidence to support the hypothesis that school closures helped bring down rates of infection among children.

In Panel B of Figure 5, we plot the pre-trend estimates obtained from regression equation (3) (the red squares) and "treatment" effects for three weeks following school closures, estimated by the imputation method of Borusyak et al. (2021) according to equation (2) (the blue dots), together with 95% confidence intervals. The figure validates the empirical design: the pre-trend coefficients are small and, with one exception, statistically insignificant from zero.[31] Moreover, the figure confirms the pattern observed in Panel A, namely that the school closures have had little impact on infection rates: the treatment effects are small and typically statistically indistinguishable from zero.

We report the corresponding treatment effects averaged over the first three weeks of the summer holiday in the first row of Table 1. The point estimate for the entire three-week period is - 0.126 (column (4)), with a 95% confidence interval of [-0.335, 0.082]. Thus, taking the uncertainty of the estimate into account, the lower bound of the confidence interval implies that the school closures have – at best – prevented 0.335 infections per 100,000 children daily. This is a rather small effect in terms of absolute magnitude. It should be noted, however, that the mean daily infection rate of children in the week before the start of the summer holiday was also very low (0.680, see column 5 of Table 1).

The Impact of School Closures on Infection Rates among Adults

Next, we turn to the impact of the school closures on SARS-CoV-2 infection rates among adults, where we distinguish between adults in the age ranges of 15-34, 35-59, and 60+. Figure 6 repeats the structure of Figure 5 for each of these groups, with rows (2) to (4) of Table 1 providing the corresponding averages. Overall, they provide little support for the hypothesis that school closures would help bring down infection rates. For example, the lower bound of the confidence interval for the most vulnerable group of adults – the population older than 60 (row (4) and column (4) in Table 1) – signifies that school closures prevented at most 0.026 infections per 100,000 per day in this group. As before, there is no evidence of pre-trends, although the precision of the pre-trend estimates tends to be low.

In Figure 7 and in row (5) of Table 1, we repeat the analysis of deaths per 100,000. Here, we restrict the analysis to adults aged 60 and above, the age category comprising 94% of all COVID-19 deaths in Germany. Not surprisingly, given our previous findings, there is no indication the closures

---

[31] It should be noted that the F-test weakly rejects the hypothesis that coefficients are jointly equal to zero with a p-value of 0.011. However, coefficients are sometimes below and sometimes above zero and do not exhibit a clear upward or downward trend.

helped prevent deaths.

To summarize, the summer closures appear to have had little impact on SARS-CoV-2 infections among children and adults. To put these results into perspective, it is important to bear in mind that schools typically operated at lower capacity before the summer holiday. Moreover, in the weeks before the start of the school holiday, SARS-CoV-2 infection rates were generally low in all states, with an incidence of around 0.7 per 100,000 inhabitants per day. In such a situation, it may not be surprising that school closures in the summer did not help reduce the infection rate further.

4.2 The Effect of School Reopenings after the Summer Holidays on the Spread of SARS-CoV-2

Having established that the school closures in the summer have had little impact on the spread of SARS-CoV-2, we turn to the impact of school reopenings on infection rates. As we described in Section 2.2, after the summer holiday schools started to operate at full capacity, although strict hygiene rules and clear procedures specifying what to do in the event of a school outbreak were introduced. The effects of the school closures and reopenings may therefore not be negatively symmetric. Moreover, there may be "anticipation" effects of school reopenings at play, driven by families returning from their vacation during the last two weeks or so of the summer holiday.

The Impact of School Reopening on Infection Rates among Children.

In Panel A of Figure 8, we display daily infection rates per 100,000 children, smoothed using a moving average filter with three lags and three leads, from June 1 until the fall school holiday started. The figure distinguishes between six groups of states with differing school reopening dates, indicated by the vertical lines. A striking pattern emerges. Infection rates among children systematically tend to increase in the two weeks before the end of the summer holiday and decline shortly after schools have reopened.

We report treatment estimates based on the imputation method by Borusyak et al. (2021) in Panel B of Figure 8, where we allow for two weeks of "anticipation effects" of school reopenings (blue dots). The estimates confirm the pattern visible in Panel A: point estimates increase and are statistically different from zero in the last two weeks of the summer holiday; they then decline from the third day of schools being open and turn negative from the second week. Pre-trend estimates *prior to* two weeks before schools reopened (red squares) are generally small in magnitude (compared with the effects on and around the treatment date) and not statistically significant

different from zero – in line with our findings that the school closures in the summer had little impact on the spread of the SARS-CoV-2 virus in the child population.[32]

While the significant negative effects in the second and third weeks after school reopenings may appear puzzling, we do not place much emphasis on this finding. The negative effects stem from the two states which reopened their schools last (Baden Wuerttemberg and Bavaria, the thin blue and green lines in Panel A of Figure 8), where cases seem to have increased four weeks before the end of the holiday rather than two. Removing these two states from our sample in Panel C of Figure 8 causes the negative effect to disappear and allows us to confirm the increase in cases before reopening, which dissipates shortly after.[33]

The fact that SARS-CoV-2 infection rates among children start to increase *before* schools reopen makes it highly unlikely that increased contact with other children, caused by the reopening of schools, is responsible for the uptick in cases among children. In our view, the most plausible explanation for the pattern of treatment effects relates to travel behavior. Families often spend their summer holiday in areas where infection rates were higher than in Germany and traveling itself is likely to increase the risk of infection. At the same time, the cost of testing was waived for returning travelers on August 1 and testing became compulsory for travelers returning from high-risk countries on August 8. Findings reported in a complementary paper by Isphording et al. (2020) support this interpretation. Drawing on proprietary data on mobile phone usage, these authors show that incoming mobility steadily grows during the last two weeks of the summer holiday and drops to a lower and stable level once schools reopen (Appendix Figure A1 in their paper). Similar patterns are not visible for outgoing mobility, supporting the association of this pattern with school holidays.

To provide further evidence on the reasons behind the increased infection rates before school reopenings, we display the evolution of the (estimated) number of PCR tests per 100,000 inhabitants in Panel A of Appendix Figure A1. Testing intensity tends to increase in the last two weeks of the summer holiday, in line with both increased testing of asymptomatic travel returnees and increased infections and symptoms among those returning from vacations. To distinguish between the two explanations, Panel B plots the evolution of the share of positive cases. If broad testing is the key mechanism, this share should decline before schools reopen, while if infections grow without a special effort to test, the share of positive cases should grow. The figure does not show a visible

---

[32] It should be noted, however, that the F-test rejects the hypothesis that coefficients are jointly equal to zero with a p-value of 0.005, which is in part related to the patterns for late-treated states described below. Note that coefficients are sometimes below and sometimes above zero and do not exhibit a clear upward or downward trend.
[33] Removing these states from our sample reduces the time horizon over which treatment effects can be reliably estimated, which is why we present treatment effects only up to 10 days before and after treatment.

change around the end of the summer holiday in either direction, suggesting that both mechanisms contributed to the temporary rise in confirmed cases before schools reopened after the summer holiday.[34]

In row (1) of Table 2 we report the treatment effects for our benchmark event studies of Figure 8, averaged over one-week periods starting from two weeks before and until three weeks after the end of the summer holiday. Columns (4) and (5) report the average daily coefficients in the second and third week after school start – by which the temporary increase due to travel behavior and increased testing should have subsided. These estimates provide no support for the conjecture that school reopenings increase the risk of infection among children (because of increased contact with other children or for other reasons).

The Impact of School Reopenings on Infection Rates among Adults

In Figure 9 we repeat the analysis for the three age groups of adults and obtain broadly similar results. The raw data displayed in Panel A shows upticks in confirmed cases before school reopenings, followed by a decline in confirmed cases during the first days of school. This again could be related to increased testing upon return from travels or a higher risk of infection during travels. This pattern is particularly visible for states in which summer holidays ended and schools reopened early (e.g., the black and dark blue lines in the figure). The estimates in Panel B of Figure 9, as well as their averages reported in rows (2) to (4) of Table 2, also show no evidence for the hypothesis that school reopenings could increase SARS-CoV-2 infection rates among adults.

In contrast to the raw data displayed in Panel A of Figure 9, and the evidence presented for children in Figure 8, estimates in Panel B of Figure 9 discern only the negative effects on confirmed cases following the reopening of schools, but not the preceding increase in cases. However, when we remove the two states that reopened schools last, like in Panel C of Figure 8, estimates become notably similar to those for children: they show an "anticipatory" increase in cases and a return to the trend within a week after the schools reopened (see Figure 10). The estimated negative effects on confirmed cases among adults observed after schools reopened appear to be driven by the pre-treatment dynamics in two states and hence cannot be considered as robust.

Figure 11 and row (5) of Table 2 further suggest that school reopenings did not increase COVID-19 related death rates among adults aged 60 and above. The upper bound of the confidence interval in the first three weeks after school reopenings in row (5), column (5) of Table 2 implies that daily, at most, 0.014 deaths per 100,000 older adults could have been prevented had schools

---

[34] Statistical analysis on these data is difficult as the data are defined at the aggregate state level.

remained closed.

Heterogenous Effects by Baseline Infection Levels and Population Density

The period of the summer holiday end is interesting in that infection rates were still low in some districts but considerably higher in others (although still relatively low compared with the fall of 2020). Reopening the schools may have had different impacts in those districts. To investigate the possibility, we show in Figure 12 the effects of summer holiday reopenings on SARS-CoV-2 infection rates separately for districts with below and above median infection rates in the third week before the end of the summer holiday (corresponding to the threshold of 5.52 infections per 100,000 inhabitants per week). We find no evidence that school reopenings accelerated the spread of SARS-CoV-2 among children or adults aged 60 and above (or any other adult group, not reported for brevity) in either type of district. Thus, schools appear to have played a limited role in the transmission of SARS-CoV-2 not only in districts with very low initial infection rates, but also in districts with higher initial infection rates. Interestingly, the temporary increase in infection rates prior to the start of school is stronger in districts with higher infection rates.

Splitting the sample instead by the population density in the district, as a potential determinant of the dynamic of the spread, reveals a similar pattern (Figure 13). Schools do not lead to an increase in cases in either low- or high-density districts, while the temporary increase in infection rates in the last two weeks of the summer holidays occurs only in districts with above median population density.

4.3 The Effect of Fall School Closures on the Spread of SARS-CoV-2

We further investigate the possibility that schools prove more effective at containing the spread of SARS-CoV-2 in a high-infection environment by using the fall holidays in Germany, as they were also staggered across states and fell into a period of higher aggregate infection levels of 3.3 new reported cases per day and per 100,000 in the week before the start of the fall holiday (compared to 0.4 and 2.0 in the third week before the end of the summer holidays in low and high infection districts). The second advantage the fall holidays offer is that traveling is much less prevalent during this time, both because of the government advice against it and because the vacation is substantially shorter. A disadvantage, however, is that due to their short length and the more limited variation in timing across states, we cannot reliably estimate the effects beyond two weeks from the start of the fall holiday and, even over this time period, estimates are less precise than for the summer school closures and reopenings.

The Impact of Fall School Closure on Infection Rates Among Children

In Panel A of Figure 14, we again plot the smoothed daily infection rates per 100,000 children, starting from one week after the school reopening after the summer holiday up until the end of the fall holiday (or our sample period on October 28). The figure distinguishes among five groups of states with differing school closure dates, indicated by the vertical lines. The figure shows no clear change in infection rates after the holiday starts in any state. A noticeable feature of the figure is that, from October 1 onwards, infection rates among children increase at a considerably faster pace in the state of Bavaria, the last state to start the fall holiday (the thin green line), than in the other states. Abstracting from this outlier, the development of infection rates over time is parallel across states both preceding and during the fall holiday. Since Bavaria clearly exhibits a different trend from the other states prior to the holiday, we drop it from the remaining analysis.

In Panel B of Figure 14, we display both pre-trend estimates obtained from regression equation (3) (the red squares) and "treatment" effects for two weeks following school closures, estimated via the imputation method of Borusyak et al. (2021) according to equation (2) (the blue dots). We report corresponding point estimates, averaged over a one- and two-week windows in row (1) of Table 3. The figure and table provide little support for the hypothesis that the school closures in the fall had a containing effect on the spread of SARS-CoV-2 among children. Point estimates are not significantly different from zero. Taking the uncertainty around our point estimates into account, the lower bound of the 95% confidence interval in row (1), column (1) of the table indicates that fall school closures have prevented at most 1.279 cases per day and per 100,000 children during the first week of the holiday. This effect can be referenced against the average case rate of 4.093 (per day per 100,000) during the week before the holiday.

The Impact of Fall School Closure on Infection Rates Among Adults

In Figure 15, we repeat the analysis for the three groups of adults. The raw data in Panel A of the figure shows a clear uptick in cases among all adult groups that starts in all groups of states at around the same time, around October 1. No apparent shift in trends can be detected from the figure after the starts of the fall holidays across the groups of states. The treatment effects from the imputation estimator displayed in Panel B of Figure 15 and rows (2) to (4) of Table 3 reveal no significant effects on infection rates among adults. For example, the lower bound of the 95% confidence interval in column (1) and row (4) suggests that at most 0.584 cases per day and per 100,000 adults above 60 have been prevented during the first week of the fall holiday (with the

mean incidence rate of 3.141 cases per day per 100,000 during the week before the holiday).[35] Figure 16 and row (5) of Table 3 repeat this analysis for deaths in the 60+ age bracket, again finding no evidence for the effect of school closures on this outcome.

Taking stock, the results for the fall holidays both reinforce and complement our findings from studying the summer holidays. As for the summer holidays, we do not find school closures in the fall to have had a significant containing effect, even though the initial levels of infections were considerably higher than in the summer.

4.4 Robustness

We now check robustness of our baseline results to using alternative estimation methods, adding controls, and using a restricted sample.

We first adopt the conventional event study methodology, which involves estimating the following equation via OLS under the implicit assumption of constant treatment effects:

$$Y_{it} = \alpha_i + \beta_t + \sum_{h=-K}^{L} \tau_h 1[t = E_i + h] + \varepsilon_{it}. \tag{4}$$

Here K is the number of treatment leads, and the effects K or more days before treatment are assumed to be zero. Focusing on the effects in the first L days after treatment, we drop observations with $t > E_i + L$ (which is preferable to the common alternative of "binning" them together; see Borusyak et al., 2021). Appendix Figures B1 (for summer school closures), B2 (for summer school reopenings) and B3 (for fall school closures) support the conclusion from our benchmark estimation that schools are not major spreaders of SARS-COV-2.

Second, we note that parallel trends in levels may not hold if there are national trends in infection rates that affect districts proportionately rather than additively. In that case, the following multiplicative model may be more appropriate:

$$E[Y_{it} \mid \alpha_i, \beta_t] = \exp(\alpha_i + \beta_t + \tau_{it} D_{it}). \tag{5}$$

While, in principle, one could estimate a log-linear specification, it appears infeasible in our application as there are many district-day pairs for which no COVID-19 cases were recorded. We therefore use the Poisson Pseudo-Maximum Likelihood (PPML) method, appropriate for this assumption (e.g. Santos Silva and Tenreyro, 2006), and use the PPML-HDFE estimator of Correia et al. (2020) which allows for high-dimensional fixed effects. Since robustness of PPML methods to treatment effect heterogeneity has not been studied to date, and since robust estimators are not

---

[35] In this analysis we continue to drop Bavaria for consistency with Figure 14.

available, we use the event study formulation analogous to equation (4). Estimates presented in Appendix Figures C1-C3 are once again similar to our benchmark estimates.

Third, de Chaisemartin and D'Haultfœuille (2020) propose an alternative robust estimator that allows for heterogenous treatment effects in a staggered difference-in-difference setting. This method differs from that proposed by Borusyak et al. (2021) in terms of the nontreated comparison group it leverages. For an observation h periods after treatment only the period just before treatment is used as a comparison, while the Borusyak et al. (2021) estimator exploits parallel trends fully, using all pre-treatment periods. The approach to pre-trend testing is also different, as de Chaisemartin and D'Haultfœuille (2020) do not make a conceptual distinction between the post-treatment effects and the pre-trends. In Appendix Figures D1-D3 we display point estimates based on the de Chaisemartin and D'Haultfœuille (2020) method.[36] For the summer school reopenings, we account for the possibility of anticipation effects by shifting the treatment event as if it happens 14 days earlier. We find estimates that are in line with those based on the Borusyak et al. (2021) method, even though their statistical precision cannot be assessed.

We next control for several factors that may influence transmission of SARS-CoV-2 and which we abstract from in our main specification. First, high temperatures are believed to create less suitable conditions for the virus to spread (Mecenas, 2020). We, therefore, include the local average daily temperature as a control at the imputation stage (such that its coefficient is estimated purely from non-treated observations). Second, the spread of the virus, regardless of the schools, may differ in tourist destinations. To capture this, we construct two measures of tourist intensity and control for their interactions with the day indicators. Specifically, we measure the number of guest arrivals in accommodation facilities per capita prior to the pandemic (in 2019) and exposure to a nearby international airport, as described in Section 2.3. Finally, confirmed cases tend to exhibit a systematic within-week pattern, which may differ across states. We therefore control for the day of the week, interacted with district fixed effects. As Appendix Figures E1-E3 show, adding all controls together has little impact on our estimates. Results are also unchanged in unreported results where these controls are added sequentially.

Finally, we consider restricting the sample by eliminating most popular holiday travel destinations, as measured in terms of guest arrivals per capita in 2019. The associated coefficient plots in Appendix Figure F1 again confirm robustness of our results.

---

[36] We are unfortunately not able to provide standard errors for them as analytical standard errors are not available for them, while bootstrap proposed by de Chaisemartin and D'Haultfœuille is too computationally intensive for the size of our dataset.

5   Conclusion

This paper contributes to the exponentially growing literature on the role of schools in transmission of SARS-CoV-2 by providing quasi-experimental evidence. In contrast to the studies of outbreaks in selected schools, this paper informs about the aggregate effects of school closures with country-wide data. We leverage the variation in the timing of the summer and fall holidays across the 16 states of Germany and apply the imputation estimator recently developed by Borusyak et al. (2021) for such staggered settings.

We find that schools play a subordinate role in the spread of SARS-CoV-2, suggesting that the benefits of their closures may not outweigh the costs. The summer school closures do not appear to have had a containing effect on infections in either the school population or older generations. Similarly, an analysis of the impact of fall holiday closures allows us to evaluate whether closures are more effective in more advanced stages of the pandemic. Our results suggest they are not: the fall closures do not appear to have significantly impacted infections among children and adults, although the confidence intervals for the fall estimates are wider and do not allow us to reject the possibility of some sizable effects.

In line with our results on school closures, we find concerns about the return to full schooling capacity after the summer holidays to be unsubstantiated: infections among children and adults did not rise with the start of the new academic year. Instead, infections appear to increase in the last weeks of the summer holidays and *decline* in the days after reopening. The result is robust to a series of specification checks and is in our view likely to be driven by increased testing and a higher risk of infection of families returning home from their travels shortly before the summer holidays ended.

We acknowledge that our study period precedes the emergence of allegedly more transmissible variants of the virus, such as the (British) B.1.1.7 strain and precedes vaccination efforts — both of which are likely to affect the transmission risk in schools, though in opposite directions. We further recognize that our findings may not carry over to countries with different regulations regarding the operation of schools or different climate.

While it is not our domain of expertise to explain *why* schools appear to have played a subordinate role on the spread of SARS-CoV-2 over the summer and fall, epidemiological studies hint at several potential explanations. One possibility is that the measures introduced in German schools to avoid contagion have been effective. Alternatively, children could be less susceptible to infection (Davies et al., 2020), or less contagious than adults because of the smaller exhaled air

volume and higher probability of an asymptomatic course of the disease (Jones et al., 2020).[37] Further epidemiological evidence on the relative role of such mechanisms would complement the findings of this paper.

---

[37] An asymptomatic course of the disease reduces the risk of spreading the virus, for instance by coughing (Jones et al., 2020).
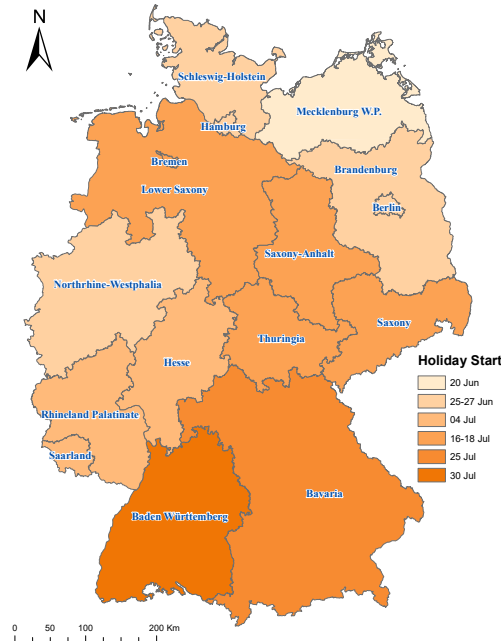
Figures

## Figure 1: School Holidays in Federal Germany

Panel A: The Summer Holidays

Panel B: The Fall Holidays
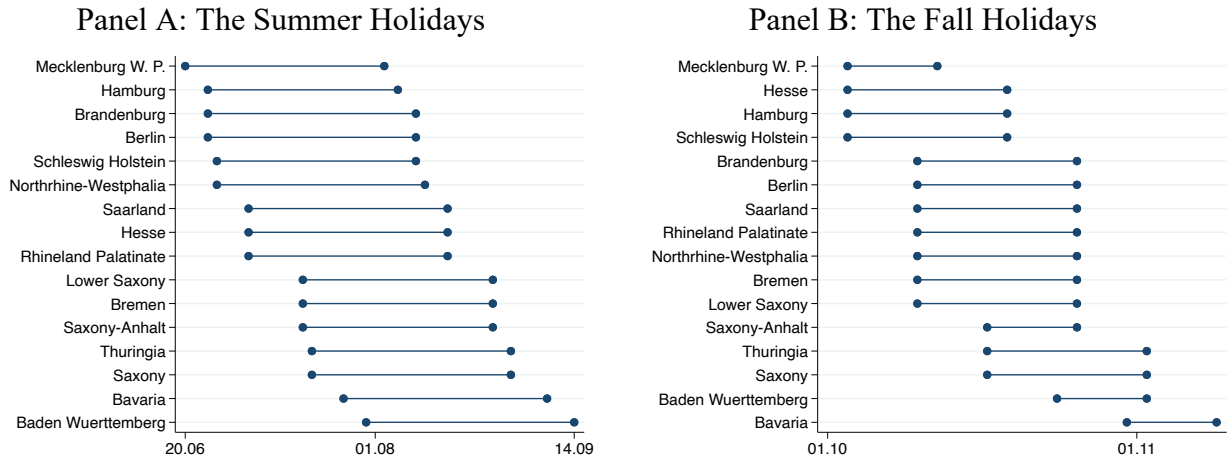
Note: This figure displays the first day of the official school holidays in German states and the first day when schools reopened after the holiday. Panel A corresponds to the summer holidays while Panel B to the fall holidays. We include the preceding weekend when the official holiday start falls on a Monday. The difference between the start and end dates ranges between 42 and 46 days in the summer and between 9 and 16 days in the fall.

Figure 2: Map of Germany and the Starting Dates of the Summer Holiday

Note: This map of Germany indicates the starting dates of the summer holiday in Germany. The colour of each state is darker, the later the start of the school holiday. Some starting dates are grouped as indicated in the legend.

Figure 3: The Course of the Pandemic: Germany in International Comparison

A: Daily Cases per 100k	B: Daily Deaths per 100k
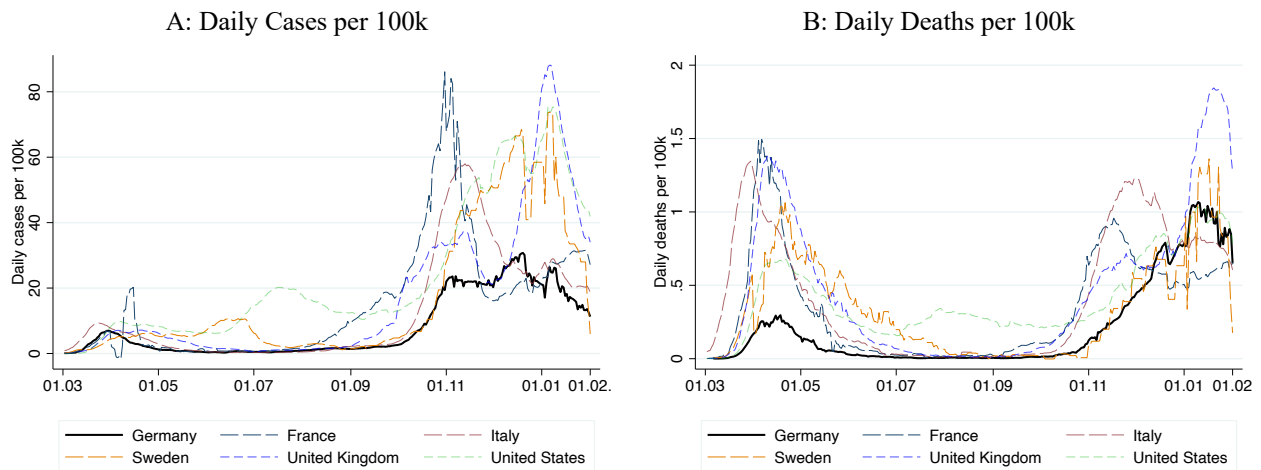
Note: This figure displays the daily new confirmed cases (Panel A) and deaths (Panel B) per 100,000 inhabitants in Germany, France, Italy, Sweden, United Kingdom, and the United States. The lines in both panels are smoothed using a uniformly weighted moving average filter with three lags and three leads. Data source (in this figure only): the European Centre for Disease Prevention and Control (ECDC).

Figure 4: SARS-CoV-2 Incidence by Age Bracket in Germany
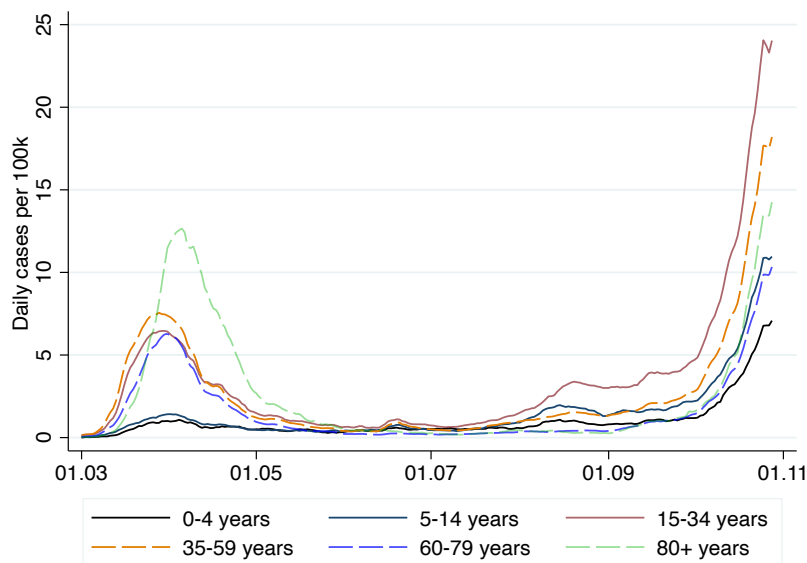
Note: Figure 4 displays the daily new cases per 100,000 over time in six available age brackets respectively: 0-4 years, 5-14 years, 15-35 years, 35-59 years, 60-79 years, and 80+ years. The lines are smoothed using a uniformly weighted moving average filter with three lags and three leads. Data source: RKI.

Figure 5: The Impact of the Summer School Closures on Children of Age 5-14

A: Raw Data

B: Estimates

Note: Panel A displays the daily cases per 100,000 in the age bracket 5-14 years, smoothed with a uniformly weighted moving average filter including three lags and three leads. The districts are grouped according to the holiday starting date, and the data are shown until schools reopened after the summer holiday. Panel B displays the treatment effect estimates using the Borusyak et al. (2021) imputation estimator including district and day fixed effects (blue squares, following equation (2)), as well as OLS estimates for pre-trends (red squares, following equation (3)). The outcome variable is defined as the number of daily reported COVID-19 cases (per 100,000 in the age bracket 5-14 years), and the districts are weighted according to the population in the age bracket 5-14 years. The event is defined as the first day of the summer holiday, and the estimation sample includes all observations from June 1 and until the summer holidays end. The shadows reflect the range inside the 95% coefficient interval, with standard errors clustered at the NUTS-2 level (38 clusters).

Figure 6: The Impact of the Summer School Closures on Other Age Brackets

A: Raw Data   B: Estimates

Age Bracket: 15-34

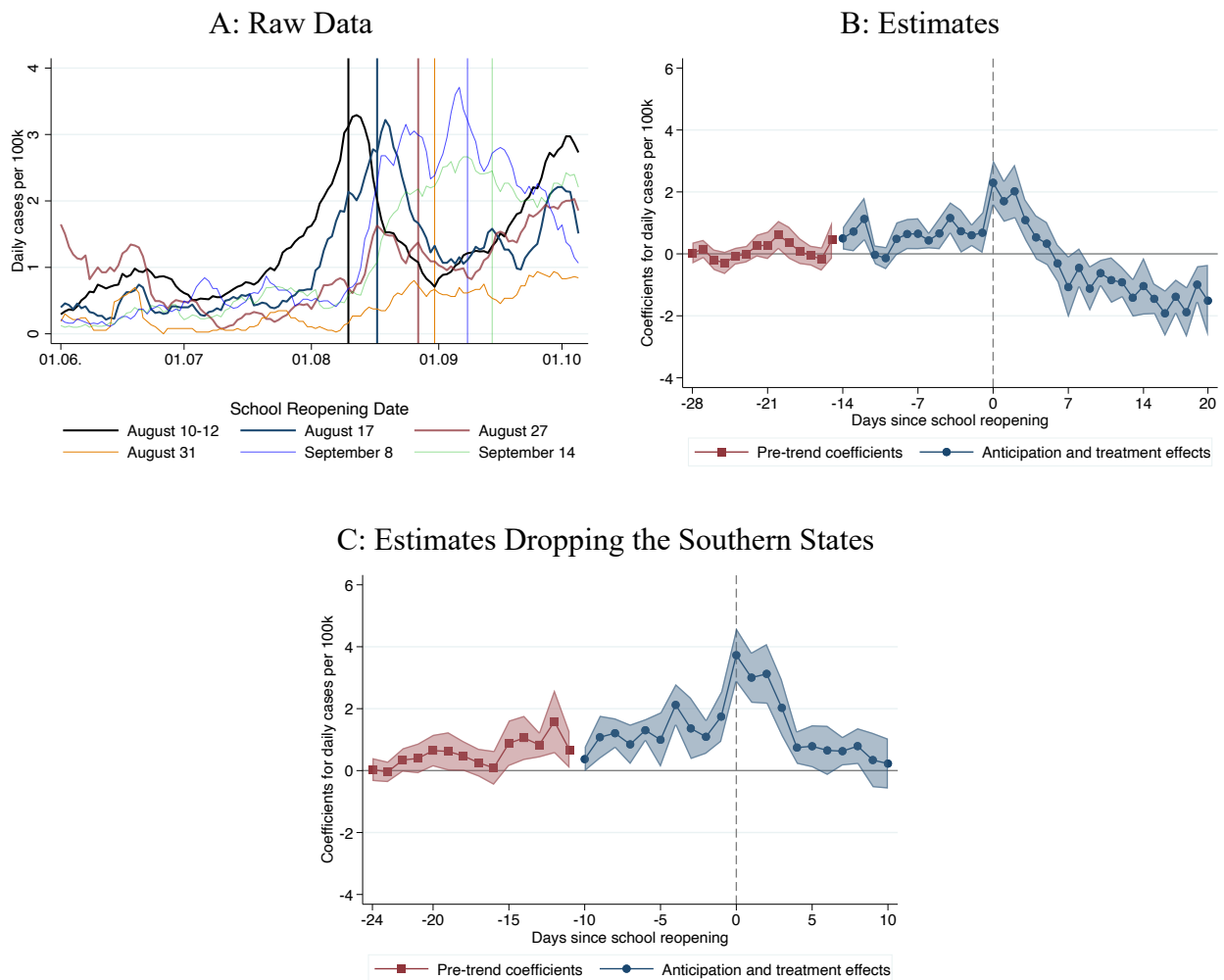### Age Bracket: 35-59

Age Bracket: 60+

Note: Panel A displays the daily cases per 100,000 in the respective age brackets, smoothed with a uniformly weighted moving average filter including three lags and three leads. The districts are grouped according to the holiday starting date, and the data are shown until schools reopened after the summer holiday. Panel B displays the treatment effect estimates using the Borusyak et al. (2021) imputation estimator including district and day fixed effects (blue dots), as well as OLS estimates for pre-trends (red squares). The outcome variable is defined as the number of daily reported COVID-19 cases (per 100,000 in the respective age bracket), and the districts are weighted according to the age-bracket specific population. The event is defined as the first day of the summer holiday, and the estimation sample includes all observations from June 1 until the summer holidays end. The shadows reflect the range inside the 95% coefficient interval, with standard errors clustered at the NUTS-2 level (38 clusters).

Figure 7: The Impact of the Summer School Closures on Deaths, Age Group 60+

Note: Panel A displays the daily deaths per 100,000 in the respective age brackets, smoothed with a uniformly weighted moving average filter including three lags and three leads. The districts are grouped according to the holiday starting date, and the data are shown until schools reopened after the summer holiday. Panel B displays the treatment effect estimates using the Borusyak et al. (2021) imputation estimator including district and day fixed effects (blue dots, following equation (2)), as well as OLS estimates for pre-trends (red squares, following equation (3)). The outcome variable is defined as the number of COVID-19 deaths attributed to the reporting date (per 100,000) in the age bracket 60+, and the districts are weighted according to population in the age bracket 60+. The event is defined as the first day of the summer holiday, and the estimation sample includes all observations from June 1 and until the summer holidays end. The shadows reflect the range inside the 95% coefficient interval, with standard errors clustered at the NUTS-2 level (38 clusters).

Figure 8: The Impact of the Summer School Reopenings on Children of Age 5-14

A: Raw Data

B: Estimates

### C: Estimates Dropping the Southern States

Note: Panel A displays the daily cases per 100,000 in the age bracket 5-14 years, smoothed with a uniformly weighted moving average filter including three lags and three leads. The districts are grouped according to the school reopening date, and the data after October 5 and after the fall holiday starts are not shown. Panel B displays the anticipation and treatment effect estimates using the Borusyak et al. (2021) imputation estimator including district and day fixed effects (blue dots, following equation (2)), as well as OLS estimates for pre-trends (red squares, following equation (3)). Anticipation effects are allowed within 14 days before schools reopened. The outcome variable is defined as the number of daily reported COVID-19 cases (per 100,000 in the age bracket 5-14 years) and the districts are weighted according to the population in the age bracket 5-14 years. The event is defined as the first day after the summer holiday, and the estimation sample includes all observations from June 1 and until the fall holiday begins. The shadows reflect the range inside the 95% coefficient interval, with standard errors clustered at the NUTS-2 level (38 clusters). Panel C displays the results from the same specification as in Panel B, with the exception that we drop the districts in Bavaria and Baden Wuerttemberg from the sample and allow for anticipation and treatment effects only 10 days before and 10 days after school reopening.

Figure 9: The Impact of the Summer School Reopenings on Other Age Brackets
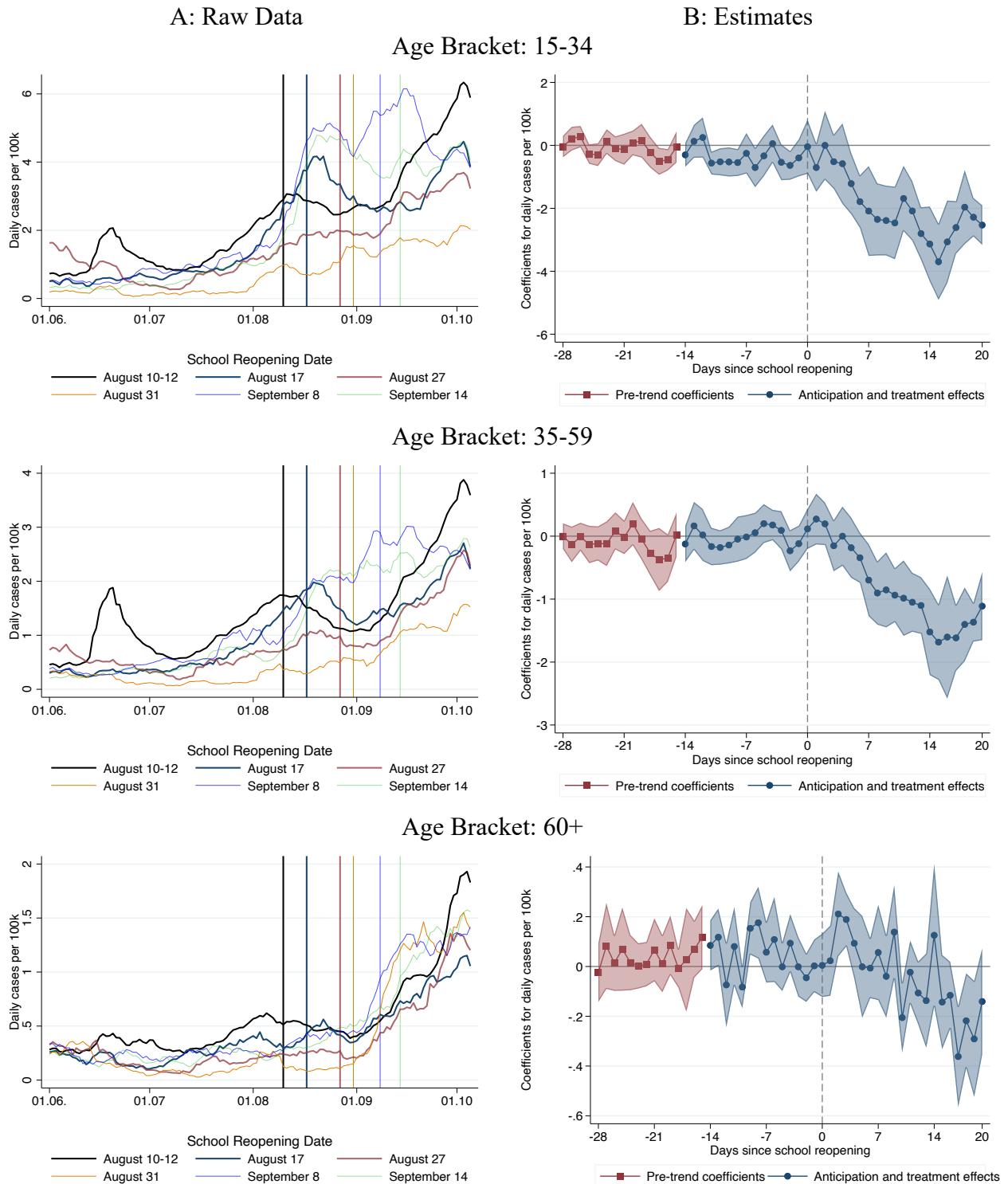
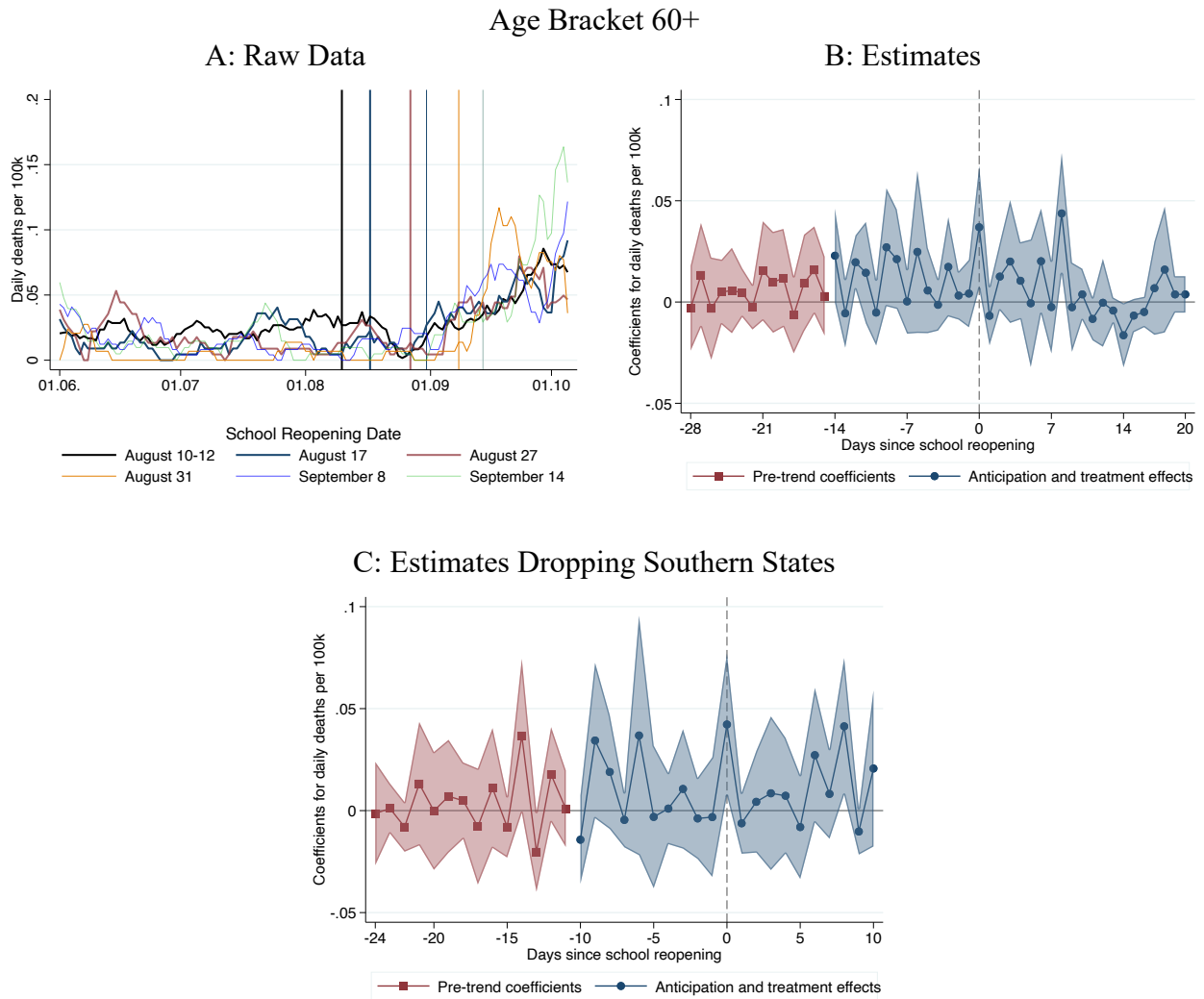### A: Raw Data

Age Bracket: 15-34

B: Estimates

Note: Panel A displays the daily cases per 100,000 in the respective age bracket, smoothed with a uniformly weighted moving average filter including three lags and three leads. The districts are grouped according to the school reopening date, and the data after October 5 and after the fall holiday starts are not shown. Panel B displays the anticipation and treatment effect estimates using the Borusyak et al. (2021) imputation estimator including district and day fixed effects (blue dots), as well as OLS estimates for pre-trends (red squares). Anticipation effects are allowed within 14 days before schools reopen. The outcome variable is the number of daily COVID-19 cases (per 100,000 in the age bracket) and the districts are weighted by the age-bracket specific population. The event is defined as the first day after the summer holiday, and the estimation sample includes all observations from June 1 and until the fall holiday begins. The shadows reflect the range inside the 95% coefficient interval, with standard errors clustered at the NUTS-2 level (38 clusters).

Figure 10: School Reopenings: Estimates Dropping Southern States

A: Age Bracket 15-34

B: Age Bracket 35-59
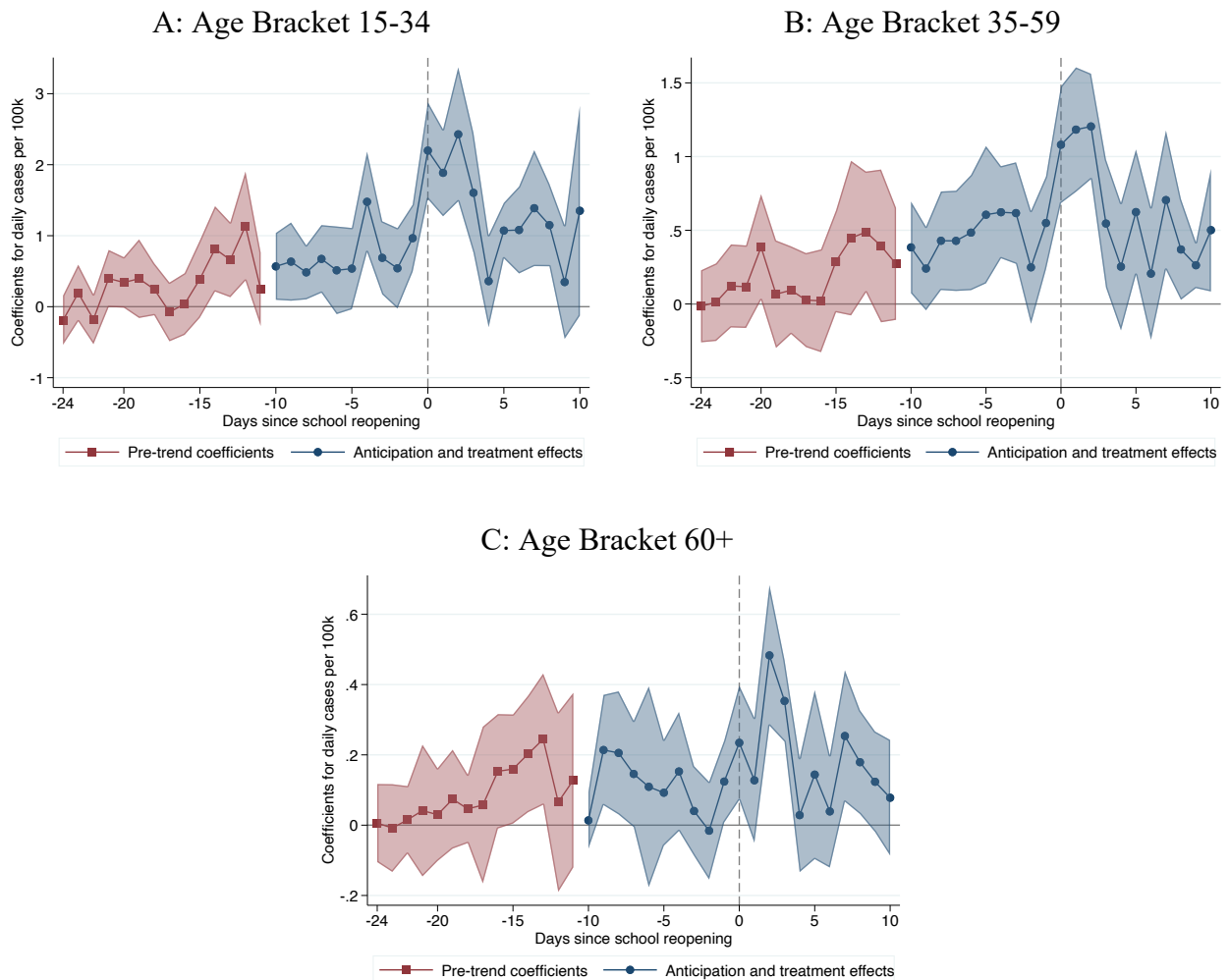
C: Age Bracket 60+

Note: The three panels, corresponding to different age brackets, display the results from the Borusyak et al. (2021) imputation estimator in specification (2) including district and day fixed effects as well as OLS estimates for pre-trends (red squares, following equation (3)), dropping the districts in Baden Wuerttemberg and Bavaria from the sample. Both anticipation and treatment effects are allowed up to 10 days relative to school reopening. The event is defined as the first day after the summer holiday, and the estimation sample includes all observations from June 1 and until the fall holiday begins. The districts are weighted by the age bracket-specific local population. The shadows reflect the range inside the 95% coefficient interval, with standard errors clustered at the NUTS-2 level (38 clusters).

Figure 11: The Impact of the Summer School Reopenings on Deaths

Age Bracket 60+

Note: Panel A displays the daily deaths per 100,000 in the age bracket 60+, smoothed with a uniformly weighted moving average filter including three lags and three leads. The districts are grouped according to the school reopening date, and the data are shown until October 5 or the day when the fall holiday starts (whichever is earlier). Panel B displays the anticipation and treatment effect estimates using the Borusyak et al. (2021) imputation estimator including district and day fixed effects (blue dots, following equation (2)), as well as OLS estimates for pre-trends (red squares, following equation (3)). Anticipation effects are allowed within 14 days before schools reopen. The outcome variable is defined as the number of daily reported COVID-19 deaths (per 100,000 in the respective age bracket) and the districts are weighted by the age bracket-specific local population. The event is defined as the first day after the summer holiday, and the estimation sample includes all observations from June 1 and until the fall holiday begins. The shadows reflect the range inside the 95% coefficient interval, with standard errors clustered at the NUTS-2 level (38 clusters). Panel C displays the results from the same specification as in Panel B, with the exception that we drop the districts in Bavaria and Baden Wuerttemberg from the sample and allow for anticipation and treatment effects only 10 days before and 10 days after school reopening.

Figure 12: School Reopenings: Heterogeneity in Terms of Preceding Infection Levels
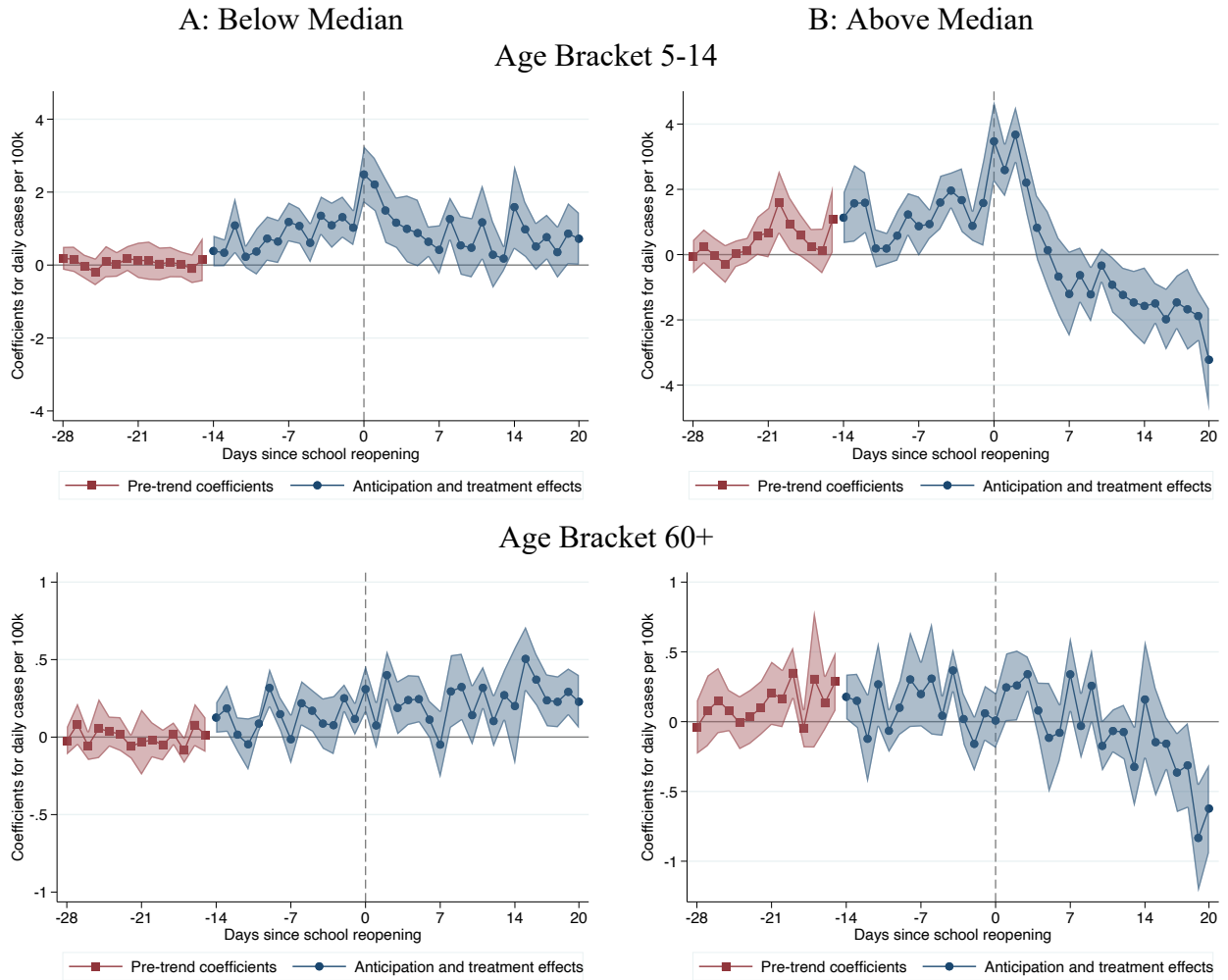
A: Below Median

B: Above Median

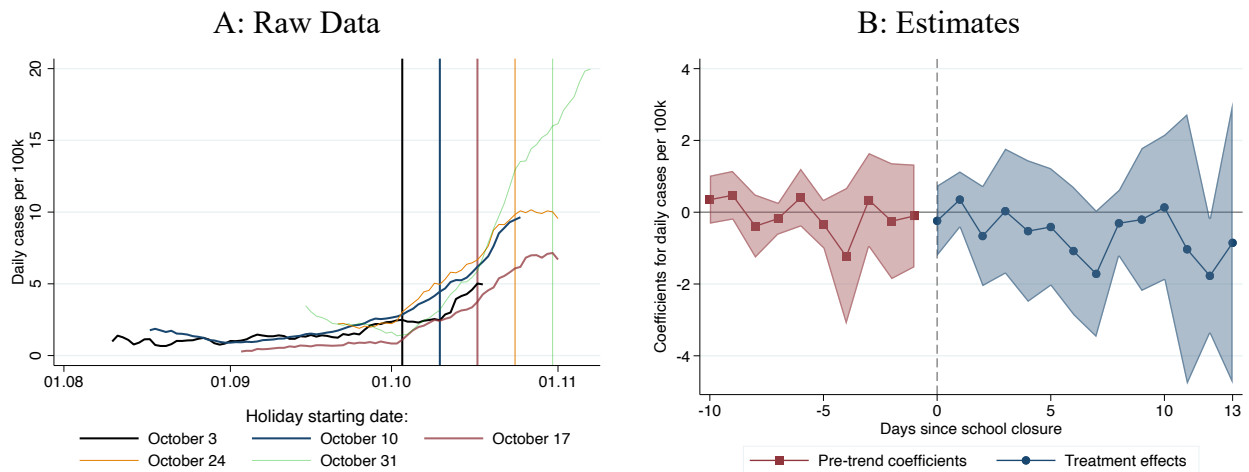#### Age Bracket 5-14

Age Bracket 60+

These figures repeat the analysis of Figures 9 and 10, Panel B, on subsamples. Panel A restricts the sample to the districts below median in terms of total daily cases per 100,000 (across all age groups) in the third week before school reopening after the summer holiday, while Panel B restricts the sample to the districts above median. Both panels display the anticipation and treatment effect estimates using the Borusyak et al. (2021) imputation estimator including district and day fixed effects (blue dots, following equation (2)), as well as OLS estimates for pre-trends (red squares, following equation (3)). Anticipation effects are allowed within 14 days before schools reopen. The outcome variable is defined as the number of daily reported COVID-19 cases (per 100,000 in the respective age bracket) and the districts are weighted according to the population in the age bracket 5-14 years. The shadows reflect the range inside the 95% coefficient interval, with standard errors clustered at the NUTS-2 level (38 clusters).

Figure 13: School Reopenings: Heterogeneity in Terms of Population Density
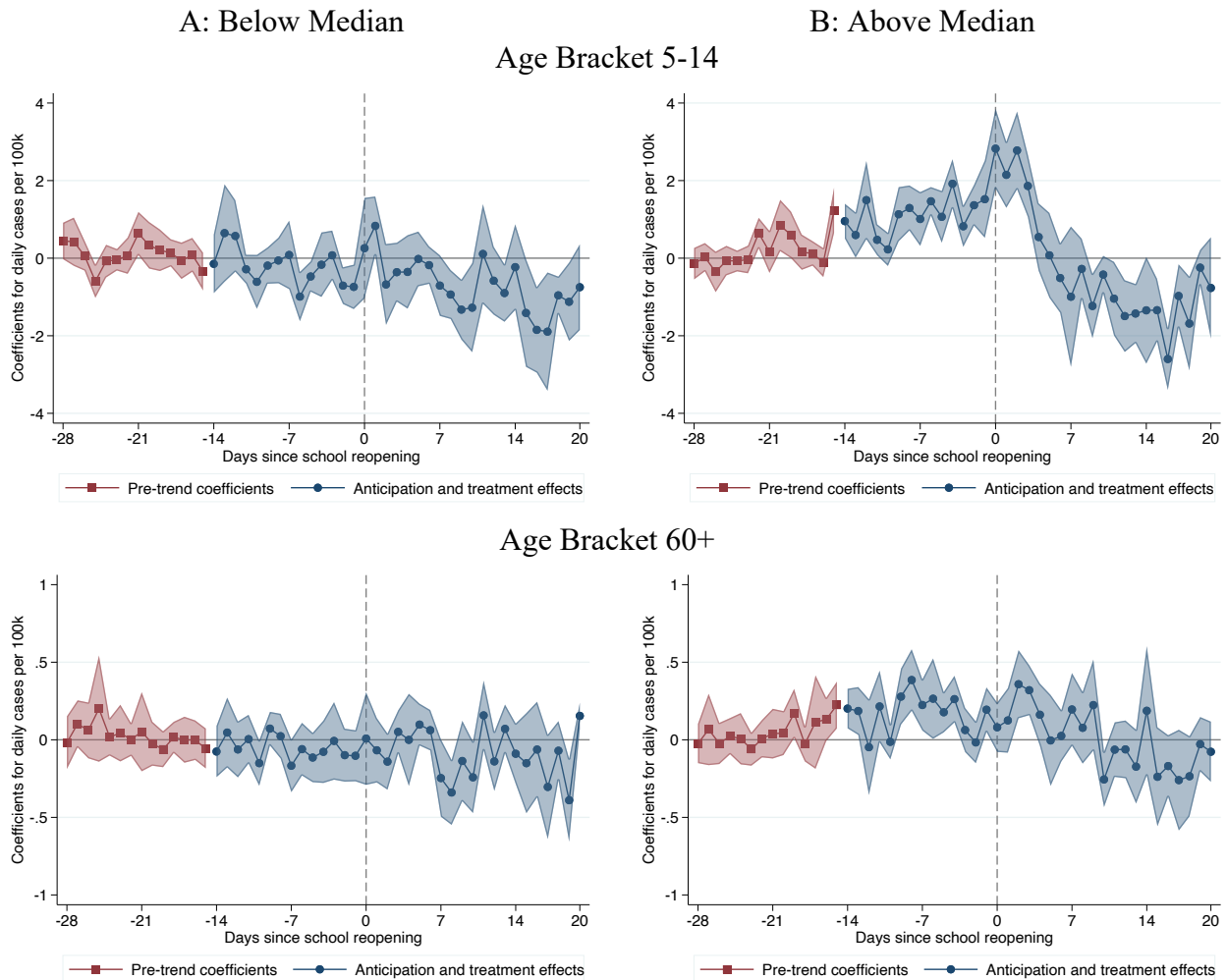
A: Below Median   B: Above Median

Age Bracket 5-14

Age Bracket 60+

These figures repeat the analysis of Figures 9 and 10, Panel B, on subsamples. Panel A restricts the sample to districts below median in terms of local population density, while Panel B restricts the sample to districts above median. Both panels display the anticipation and treatment effect estimates using the Borusyak et al. (2021) imputation estimator including district and day fixed effects (blue dots, following equation (2)), as well as OLS estimates for pre-trends (red squares, following equation (3)). Anticipation effects are allowed within 14 days before schools reopen. The outcome variable is defined as the number of daily reported COVID-19 cases (per 100,000 in the respective age bracket) and the districts are weighted according to the population in the age bracket 5-14 years. The shadows reflect the range inside the 95% coefficient interval, with standard errors clustered at the NUTS-2 level (38 clusters).

Figure 14: The Impact of the Fall School Closures on Children of Age 5-14
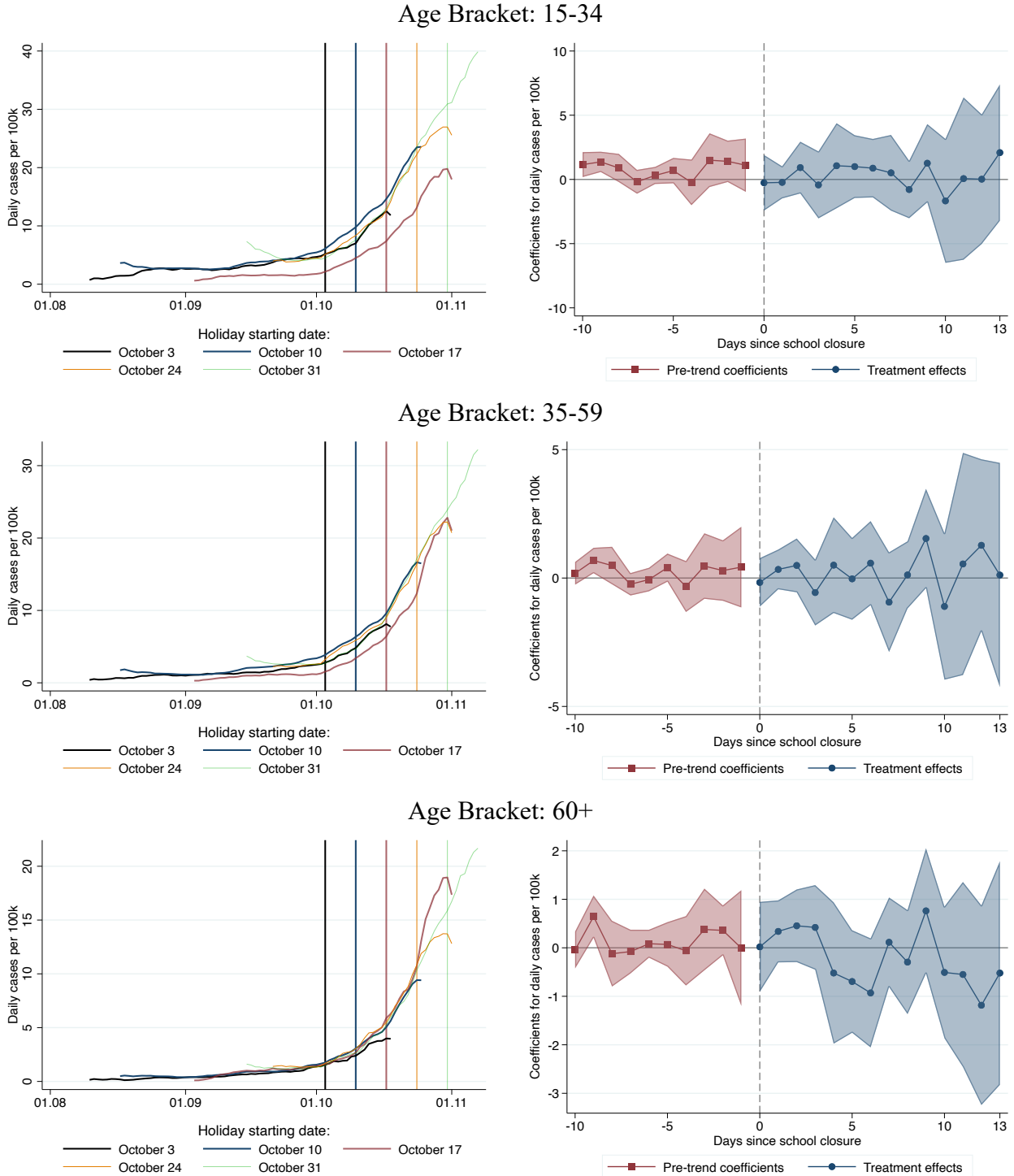

Note: Panel A displays the daily cases per 100,000 in the age bracket 5-14 years, smoothed with a uniformly weighted moving average filter including three lags and three leads. The districts are grouped according to the fall holiday starting date, and the data are shown from 7 days after schools reopened after the summer holiday and until the fall holidays end. Panel B displays the treatment effect estimates on the same sample excluding districts in Bavaria, using the Borusyak et al. (2021) imputation estimator including district and day fixed effects (blue squares, following equation (2)), as well as OLS estimates for pre-trends (red squares, following equation (3)). The outcome variable is defined as the number of daily reported COVID-19 cases (per 100,000 in the age bracket 5-14 years), and the districts are weighted according to the population in the age bracket 5-14 years. The event is defined as the first day after the fall holiday, and the estimation sample includes all observations starting 7 days after the summer holiday ends and until the fall holiday ends, or October 28 (whichever is earlier). The shadows reflect the range inside the 95% coefficient interval, with standard errors clustered at the NUTS-2 level (38 clusters).

Figure 15: The Impact of the Fall School Closures on Other Age Brackets
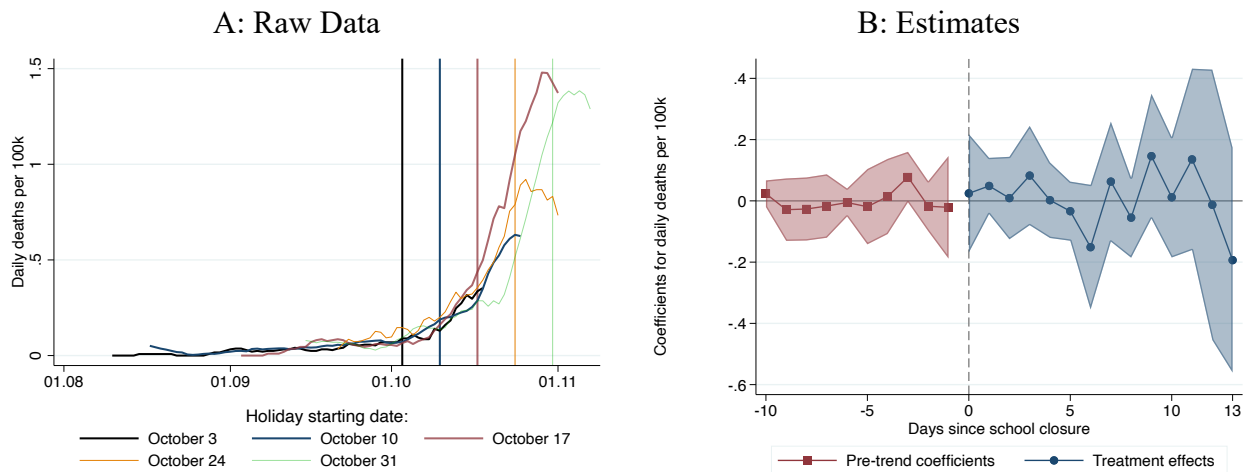
Note: Panel A displays the daily cases per 100,000 in the respective age bracket, smoothed with a uniformly weighted moving average filter including three lags and three leads. The districts are grouped according to the fall holiday starting dates. Panel B displays the anticipation and treatment effect estimates on the same sample excluding districts in Bavaria, using the Borusyak et al. (2021) imputation estimator including district and day fixed effects (blue dots), as well as OLS estimates for pre-trends (red squares). The outcome variable is the number of daily COVID-19 cases (per 100,000 in the age bracket) and the districts are weighted according to the age-bracket specific population. The event is defined as the first day after the fall holiday, and the estimation sample includes all observations starting 7 days after the summer holiday ends and until the fall holiday ends, or October 28 (whichever is earlier). The shadows reflect the range inside the 95% coefficient interval, with standard errors clustered at the NUTS-2 level (38 clusters).

Figure 16: The Impact of the Fall School Closures on Deaths, Age Group 60+

A: Raw Data

B: Estimates

Note: Panel A displays the daily deaths per 100,000 in the respective age brackets, smoothed with a uniformly weighted moving average filter including three lags and three leads. The districts are grouped according to the holiday starting date, and the data are shown from 7 days after schools reopened after the summer holiday and until the fall holidays end. Panel B displays the treatment effect estimates on the same sample excluding districts in Bavaria, using the Borusyak et al. (2021) imputation estimator including district and day fixed effects (blue dots, following equation (2)), as well as OLS estimates for pre-trends (red squares, following equation (3)). The outcome variable is defined as the number of COVID-19 deaths attributed to the reporting date (per 100,000) in the age bracket 60+, and the districts are weighted according to population in the age bracket 60+. The event is defined as the first day after the fall holiday, and the estimation sample includes all observations starting 7 days after the summer holiday ends and until the fall holiday ends, or October 28 (whichever is earlier). The shadows reflect the range inside the 95% coefficient interval, with standard errors clustered at the NUTS-2 level (38 clusters).

Tables

Table 1: Average Daily Effects of Summer School Closures

Dependent variable	Average daily effects				Mean Incidence Rate
	Week 0	Week 1	Week 2	Weeks 0-2	Week -1
	(1)	(2)	(3)	(4)	(5)
(1) Cases/100k, 5-14 years	-0.144 [-0.360, 0.072]	-0.189 [-0.410, 0.031]	-0.046 [-0.352, 0.260]	-0.126 [-0.335, 0.082]	0.680
(2) Cases/100k, 15-34 years	-0.088 [-0.288, 0.113]	-0.223 [-0.540, 0.095]	-0.309 [-0.796, 0.178]	-0.206 [-0.517, 0.104]	1.074
(3) Cases/100k, 35-59 years	-0.078 [-0.293, 0.136]	-0.281 [-0.567, 0.006]	-0.265 [-0.708, 0.178]	-0.208 [-0.510, 0.094]	0.805
(4) Cases/100k, 60+ years	0.038 [-0.015, 0.091]	0.017 [-0.053, 0.087]	0.052 [-0.053, 0.156]	0.036 [-0.026, 0.097]	0.237
(5) Deaths/100k, 60+ years	0.003 [-0.004, 0.011]	0.008 [0.000, 0.016]	0.016 [0.003, 0.029]	0.009 [0.002, 0.016]	0.010

Note: This table complements the coefficient plots from Panel B of Figures 5, 6, and 7, providing the average daily coefficients and associated 95% confidence intervals for the imputation estimator. The averages are given for weeks zero (i.e. $h = 0,\ldots,6$ days since closures; column 1), one and two (columns 2 and 3), and over the first three weeks of summer holiday (column 4) – for all age brackets and for deaths among the population aged 60+. The mean daily infection rate (per 100,000 inhabitants in the respective age group) in the seven days before schools closed in each state, weighted by the age bracket specific population, is displayed in column 5.

Table 2: Average Daily Effects of School Reopenings

Dependent variable	Anticipation effects		Average daily effects				Mean Incidence Rate
	Week -2	Week -1	Week 0	Week 1	Week 2	Weeks 0-2	Week -3
	(1)	(2)	(3)	(4)	(5)	(6)	(7)
(1) Cases/100k, 5-14 years	0.471 [0.271, 0.671]	0.702 [0.466, 0.938]	1.094 [0.647, 1.541]	-0.922 [-1.336, -0.507]	-1.455 [-1.996, -0.915]	-0.428 [-0.806, -0.050]	1.308
(2) Cases/100k, 15-35 years	-0.298 [-0.570, -0.025]	-0.401 [-0.893, 0.090]	-0.693 [-1.534, 0.148]	-2.267 [-3.208, -1.326]	-2.756 [-3.543, -1.968]	-1.905 [-2.688, -1.122]	2.397
(3) Cases/100k, 35-59 years	-0.068 [-0.294, 0.158]	0.023 [-0.196, 0.242]	-0.014 [-0.322, 0.294]	-0.933 [-1.330, -0.535]	-1.472 [-1.916, -1.029]	-0.806 [-1.151, -0.461]	1.203
(4) Cases/100k, 60+ years	0.065 [0.008, 0.122]	0.031 [-0.031, 0.092]	0.073 [0.009, 0.138]	-0.045 [-0.124, 0.034]	-0.164 [-0.254, -0.073]	-0.045 [-0.110, 0.020]	0.359
(5) Deaths/100k, 60+ years	0.013 [0.002, 0.025]	0.008 [-0.001, 0.016]	0.013 [0.002, 0.025]	0.004 [-0.007, 0.015]	0.000 [-0.011, 0.012]	0.006 [-0.002, 0.014]	0.017

Note: This table complements the coefficient plots from Panel B of Figures 8, 9, and 11, providing the average daily coefficients and associated 95% confidence intervals for the imputation estimator. The average anticipation effects are displayed in column (1) and (2), for the two weeks prior school start respectively. The averages treatment effects are given for weeks zero (i.e. $h = 0, \ldots, 6$ days since school reopening), one, and two (columns 3-5), and over the first three weeks of summer holiday (column 6) – for all age brackets and for deaths among the population aged 60+. The mean daily infection rate (per 100,000 inhabitants in the respective age group) in the third week before schools reopened in each state, weighted by the age-bracket specific population, is displayed in column 7.

Table 3: Average Daily Effects of the Fall Closures

Dependent variable	Average daily effects			Mean Incidence Rate
	Week 0	Week 1	Weeks 0-1	Week -1
	(1)	(2)	(3)	(4)
(1) Cases/100k, 5-14 years	-0.364	-0.823	-0.639	4.093
	[-1.279, 0.552]	[-2.398, 0.752]	[-1.908, 0.631]	
(2) Cases/100k, 15-34 years	0.420	0.213	0.341	8.743
	[-1.299, 2.139]	[-2.823, 3.248]	[-2.138, 2.819]	
(3) Cases/100k, 35-59 years	0.163	0.222	0.208	5.694
	[-0.782, 1.108]	[-1.986, 2.431]	[-1.444, 1.859]	
(4) Cases/100k, 60+ years	-0.131	-0.312	-0.238	3.141
	[-0.584, 0.323]	[-1.506, 0.882]	[-1.095, 0.618]	
(5) Deaths/100k, 60+ years	-0.003	0.014	0.006	0.183
	[-0.072, 0.067]	[-0.124, 0.151]	[-0.085, 0.097]	

Note: This table complements the coefficient plots from Panel B in Figures 12 and 13, providing the average daily coefficients and associated 95% confidence intervals for the imputation estimator. The averages are given for weeks zero (i.e. $h = 0, \ldots, 6$ days since closures, column 1), one (column 2) and over the first two weeks of fall holiday (column 3) – for all age brackets. The mean daily infection rate (per 100,000 inhabitants in the respective age group) in the seven days before schools closed in each state, weighted by the age bracket specific population, is displayed in column 4.

Bibliography

Adda, J. (2016). Economic Activity and the Spread of Viral Diseases: Evidence from High Frequency Data. *The Quarterly Journal of Economics*. 131 (2), 891–941.

Alon, T.; Doepke, M.; Olmstead-Rumsey, J.; Tertilt, M. (2020). *This Time It's Different: The Role of Women's Employment in a Pandemic Recession*. IZA Discussion Paper No. 13562.

Andrew, A.; Cattan, S.; Costa-Dias, M.; Farquharson, C.; Kraftman, L.; Krutikova, S.; Phimister, A.; Sevilla, A. (2020): *Learning during the Lockdown: Real-Time Data on Children's Experiences during Home Learning.* IFS Briefing Note BN288.

Auger, K. A., Shah, S. S., Richardson, T., Hartley, D., Hall, M., Warniment, A., Timmons, K.; Bosse, D.; Ferris, S. A.; Brandy, P. W.; Schondelmeyer, A. C.; Thomson, J. E. (2020). Association between Statewide School Closure and COVID-19 Incidence and Mortality in the US. *Jama.* 324(9), 859-870.

Bauer, A.; Weber, E. (2020): COVID-19: How Much Unemployment was Caused by the Shutdown in Germany? *Applied Economics Letters,* 1-6.

Bayerischer Rundfunk: Jerabek, P.; Lang, J. P. (2020, August 31). Zwei Wochen Maskenpflicht im Unterricht ab Klasse 5.

Bayham, J.; Fenichel, E. (2020). The Impact of School Closure for COVID-19 on the US Healthcare Workforce and the Net Mortality Effects. *Cold Spring Harbor Laboratory Press*. 5(5), 271-278.

Berner, R. (2020, July 14). *Immunisierungsgrad geringer als erwartet – Schulen haben sich nicht zu Hotspots entwickelt.* Uniklinikum TU Dresden.

Borusyak, K.; Jaravel, X. (2017). *Revisiting Event Study Designs, with an Application to the Estimation of the Marginal Propensity to Consume*. Working Paper.

Borusyak, K.; Jaravel, X.; Spiess, J. (2021). *Revisiting Event Study Designs: Robust and Efficient Estimation*. Working Paper.

Chaisemartin, C. de; D'Haultfœuille, X. (2020). Two-Way Fixed Effects Estimators with Heterogeneous Treatment Effects. *American Economic Review*. 110 (9), 2964-2996.

Correia, S.; Guimarães, P.; Zylkin, T. Z. (2020). Fast Poisson Estimation with High-Dimensional Fixed Effects. *Stata Journal*. 20(1), 95–115.

Davies, N.; Klepac, P.; Liu, Y.; Prem, K.; Jit, M. (2020). Age-Dependent Effects in the Transmission and Control of COVID-19 Epidemics. *Nature Medicine.* 26(8), 1205-1211.

Dehning, J.; Zierenberg, J.; Spitzner, F. P.; Wibral, M.; Neto, J. P.; Wilczek, M.; Priesemann, V. (2020). Inferring Change Points in the Spread of COVID-19 Reveals the Effectiveness of Interventions. *Science*. 369(6500).

Deutschlandfunk (2020, August 27). Wir können uns Reisen in Risikogebiete nicht leisten.

Die ZEIT (2020, September 18). Die Ruhe könnte trügerisch sein. Besonders junge Menschen stecken sich an.

DWD Climate Data Center (2020). *Recent daily station observations (temperature, pressure, precipitation, sunshine duration, etc.) for Germany, quality control not completed yet, version recent*. Deutscher Wetterdienst. Last accessed: February 10, 2021.

Engzell, P.; Frey, A.; Verhagen, M. D. (2020). Learning Inequality During the COVID-19 Pandemic. *SocArXiv*: 31235.

Fateh-Moghadam, P.; Battisti, L.; Molinaro, S.; Dallago, G.; Binkin, N.; Zuccali, M. (2020). Contact Tracing During Phase I of the COVID-19 Pandemic in the Province of Trento, Italy: Key Findings and Recommendations. *medRxiv*.

Federal Government of Germany (2020, April 20). Beschlüsse von Bund und Ländern: „Wir müssen ganz konzentriert weiter machen."

Fetzer, T. (2020). *Subsidizing the Spread of COVID-19: Evidence from the UK's Eat-Out-to-Help-Out Scheme.* CAGE Working Paper.

Fontanet, A.; Tondeur, L.; Madec, Y.; Grant, R.; Besombes, C.; Jolly, N.; Fernandes Pellerin, S.; Ungeheuer, M.-N.; Cailleau, I.; Kuhmel, L.; Temmam, S.; Huon, C.; Chen, K.-Y.; Crescenzo, B.; Munier, S.; Demeret, C.; Grzelak, L.; Staropoli, I.; Bruel, T.; Gallian, P.; Cauchemez, S.; van der Werf, S.; Schwartz, O.; Eloit, M.; Hoen, B. (2020). Cluster of COVID-19 in Northern France: A Retrospective Closed Cohort Study. *medRxiv*.

Frankfurter Allgemeine Zeitung (2020, June 5). So weit öffnen die Bundesländer ihre Schulen.

Fuchs-Schündeln, N.; Kuhn, M.; Tertilt, M. (2020). *The Short-Run Macro Implications of School and Child Care Closures.* IZA Discussion Paper No. 13353.

Goldhaber, D.; Imberman, S. A.; Strunk, K. O.; Hopkins, B.; Brown, N.; Harbartkin, E.; Kilbride, T. (2021). To What Extent Does In-Person Schooling Contribute to the Spread of COVID-19? Evidence from Michigan and Washington. NBER Working Paper No. 28455.

Goodman-Bacon, A. (2020). *Difference-in-Differences with Variation in Treatment Timing*. NBER Working Paper No. 25018.

Handelsblatt (2020, August 3). Ferienende: Wie die Bundesländer ihre Schulen wieder öffnen.

Harris, D. N.; Ziedan, E.; Hassig, S. (2021). *The Effects of School Reopenings on COVID-19 Hospitalizations*. REACH Working Paper.

Heald-Sargent, T.; Muller, W.; Zheng, X.; Rippe, J.; Patel, A.; Kociolek, L. (2020). Age-Related Differences in Nasopharyngeal Severe Acute Respiratory Syndrome Coronavirus 2 (SARS-CoV-2) Levels in Patients with Mild to Moderate Coronavirus Disease 2019 (COVID-19). *JAMA Pediatrics.* 174(9): 902–903.

Isphording, I.; Lipfert, M.; Pestel, N. (2020). *School Reopenings after Summer Breaks in Germany Did Not Increase SARS-CoV-2 Cases*. IZA Discussion Paper No. 13790.

Jones, T.; Mühlemann, B.; Veith, T.; Biele, G.; Zuchowski, M.; Hoffmann, J.; Stein, A.; Edelmann, A.; Corman, V.; Drosten, C. (2020). An Analysis of SARS-CoV-2 Viral Load by Patient Age. *MedRxiv:* 1101.

Ladhani, S. (2021). Prospective Active National Surveillance of Preschools and Primary Schools for SARS-CoV-2 Infection and Transmission in England, June 2020. *Available at SSRN 3764198.*

Liu, Y.; Morgenstern, C.; Kelly, J., Lowe, R.; Jit, M. (2021). The Impact of Non-Pharmaceutical Interventions on SARS-CoV-2 Transmission Across 130 Countries and Territories. *BMC Medicine*. 19(1), 1-12.

Macartney, K., Quinn; H. E., Pillsbury; A. J., Koirala; A., Deng; L., Winkler; N., Katelaris; A. L.; O'Sullivan, M. V. N.; Dalton, C.; Wood, N.; Brogan, D.; Glover, C.; Dinsmore, N.; Dunn, A.; Jadhav, A.; Joyce, R.; Kandasamy, R.; Meredith, K.; Pelayo, L.; Rost, L.; Saravanos, G.; Bag, S.; Corbett, S.; Staff, M.; Alexander, K.; Conaty, S.; Leadbeater, K.; Forssman, B.; Kakar, S.; Dwyer, D.; Kok, J.; Chant, K. (2020). Transmission of SARS-CoV-2 in Australian Educational Settings: A Prospective Cohort Study. *The Lancet Child & Adolescent Health*. 4(11), 807-816.

Mangrum, D.; Niekamp, P. (forthcoming) JUE Insight: College Student Travel Contributed to Local COVID-19 Spread. *Journal of Urban Economics*.

Mecenas, P., Bastos; R. T. D. R. M.; Vallinoto, A. C. R.; Normando, D. (2020). Effects of Temperature and Humidity on the Spread of COVID-19: A Systematic Review. *PLoS one*. 15(9).

Pouletty, M.; Borocco, C.; Ouldali, N.; Caseris, M.; Basmaci, R.; Lachaume, N.; Bensaid, P.; Pichard, S.; Kouider, H.; Morelle, G.; Craiu, I.; Pondarre, C.; Deho, A.; Maroni, A.; Oualha, M.; Amoura, Z.; Haroche, J.; Chommeloux, J.; Bajolle, F.; Beyler, C.; Bonacorsi, S.; Carcelain, G.; Koné-Paut, I.; Bader-Meunier, B.; Faye, A.; Meinzer, U.; Galeotti, C.; Melki, I. (2020). Paediatric Multisystem Inflammatory Syndrome Temporally Associated with SARS-CoV-2 Mimicking Kawasaki Disease (Kawa-COVID-19): A Multicentre Cohort. *Annals of the Rheumatic Diseases.* 79(8), 999–1006.

Robert-Koch Institut (2020). *Epidemiologisches Bulletin* (No. 19/2020).

Roth, J. (2020). Pre-test with Caution: Event-Study Estimates After Testing for Parallel Trends. Working Paper.

Santos Silva, J. M. C.; Tenreyro, S. (2006). The Log of Gravity. *The Review of Economics and Statistics*. 88(4), 641-658.

Strezhnev, A. (2018). *Semiparametric Weighting Estimators for Multi-Period Difference-in-Differences Designs*. Working Paper.

Sun, L; Abraham, S. (forthcoming). Estimating Dynamic Treatment Effects in Event Studies with Heterogeneous Treatment Effects. *The Journal of Econometrics*.

Tagesschau (2020a, October 10). Was gilt bei der Einreise in Deutschland?

Tagesschau (2020b, April 28). Vor den Sommerferien wieder zur Schule.

The Guardian (2020, September 7). Coronavirus cases rise steeply among young people in England.

The New York Times (2020, August 31). U.S. coronavirus rates are rising fast among children.

Ulyte, A.; Radtke, T.; Abela, I. A.; Haile, S. H.; Blankenberger, J.; Jung, R.; Capelli C.; Berger, C.; Frei, A.; Huber, M.; Schanz, M.; Schwarzmueller, M.; Trkola, A.; Fehr, J.; Puhan, M. A.; Kriemler, S. (2020). Variation in SARS-CoV-2 Seroprevalence in School-Children across Districts, Schools and Classes. *MedRxiv*.

Viner, R.; Russell, S.; Croker, H.; Packer, J.; Ward, J.; Stansfield, C.; Mytton, O.; Bonell, C.; Booy, R. (2020). School Closure and Management Practices during Coronavirus Outbreaks including COVID-19: A Rapid Systematic Review. *The Lancet Child & Adolescent Health*. 4(5), 397-404.

Vlachos, J.; Hertegård, E.; Svaleryd, H. B. (2021). The Effects of School Closures on SARS-CoV-2 among Parents and Teachers. *Proceedings of the National Academy of Sciences*. 118(9).

Wang, Z.; Zhou, Q.; Wang, C.; Shi, Q.; Lu, S.; Ma, Y.; Luo, X.; Xun, Y.; Li, W.; Baskota, M.; Yang, Y.; Zhai, H.; Fukuoka, T.; Ahn, H.; Lee, M.; Luo, X.; Liu, E., Chen, Y. (2020). Clinical Characteristics of Children with COVID-19: A Rapid Review and Meta-Analysis. *Annals of Translational Medicine*. 8(10), 620.

Yoon, Y.; Choi, G. J.; Kim, J. Y.; Kim, K. R.; Park, H.; Chun, J. K.; Kim, Y. J. (2021). Childcare Exposure to Severe Acute Respiratory Syndrome Coronavirus 2 for 4-Year-Old Presymptomatic Child, South Korea. *Emerging Infectious Diseases*. 27(2), 341.

ZDF heute (2020a, August 12). Schulstart mit Maske: Strengste Regeln in NRW.

ZDF heute (2020b, August 31). Corona Maßnahmen der Länder: Feiern, Reisen, Schule: Was jetzt wo gilt.

ZDF heute (2020c, August 5). Die Regeln der Bundesländer: Wie es zurück in die Schule geht.

The Role of Schools in Transmission of the SARS-CoV-2 Virus:
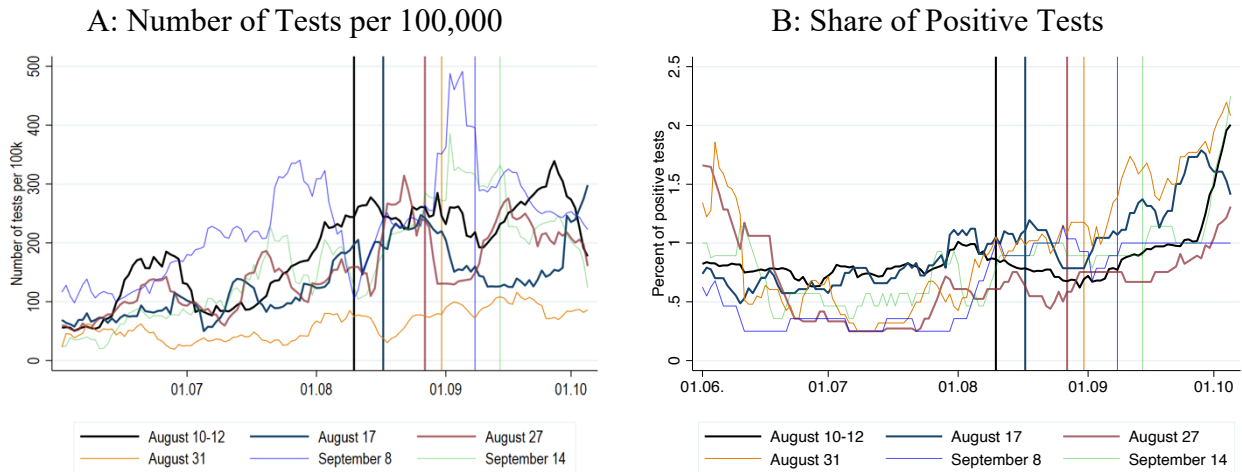# Quasi-Experimental Evidence from Germany

Clara von Bismarck-Osten[*], Kirill Borusyak[*†], and Uta Schönberg[*‡]

[*] University College London; [†] CEPR; [‡] IAB, RWI, and CReAM

March 19, 2021

## A. The Evolution of Testing over the Study Period

Figure A1: The Evolution of Testing by School Reopening Date

A: Number of Tests per 100,000   B: Share of Positive Tests

Note: Panel A displays the number of tests per 100,000 inhabitants of all age groups, inferred as the ratio of the full number of cases from our main dataset and the share of positive tests from the RKI test data described in Section 2.3. Panel B displays the percentage of positive tests. Both variables are smoothed with a uniformly weighted moving average filter including three lags and three leads, and the states are grouped according to the school reopening date after the summer holidays. Districts in Bremen and Saarland are excluded from both panels because the data are unavailable.
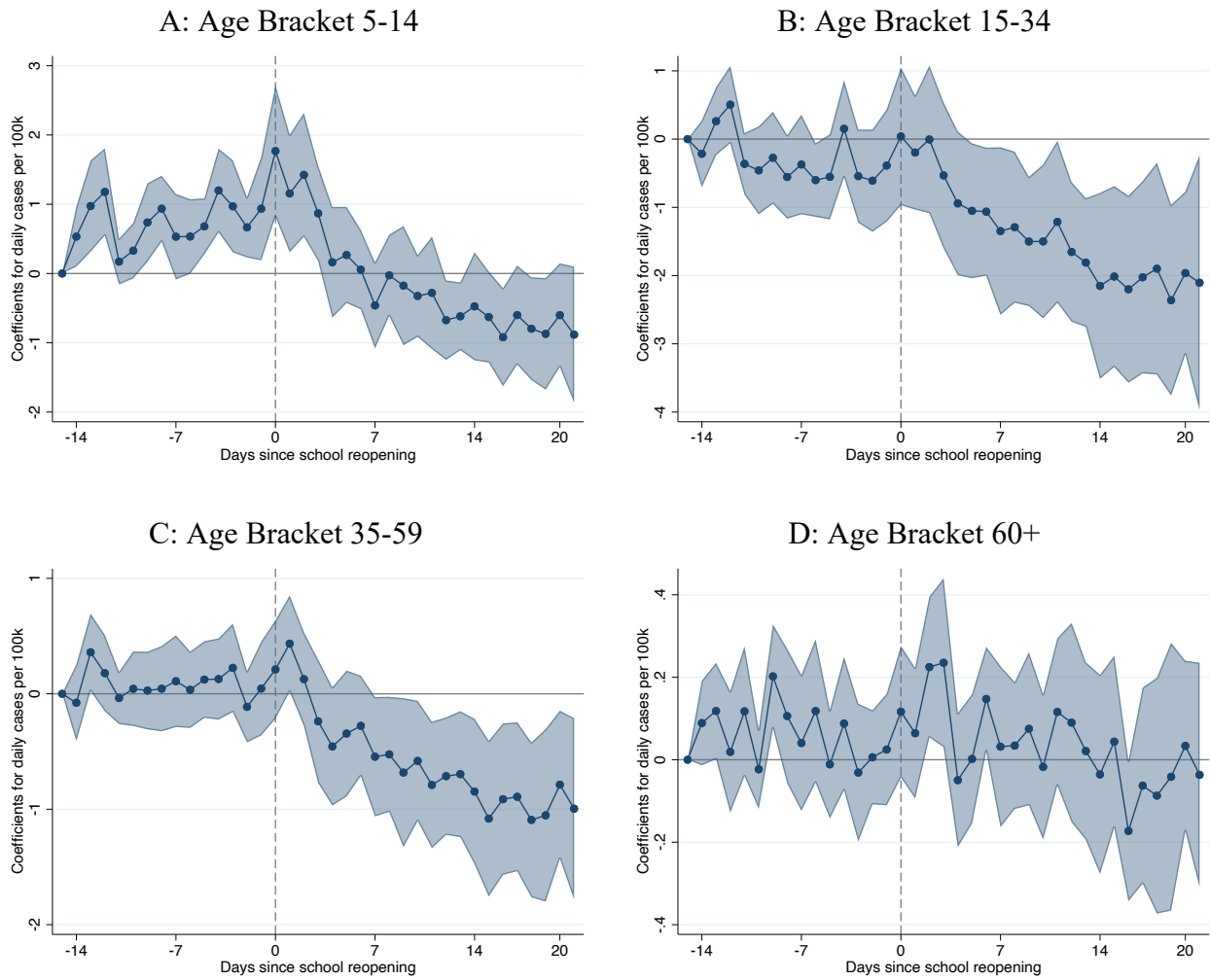
B. Estimates from Conventional Event Study

Figure B1: Summer School Closures – Estimates from Conventional Event Study
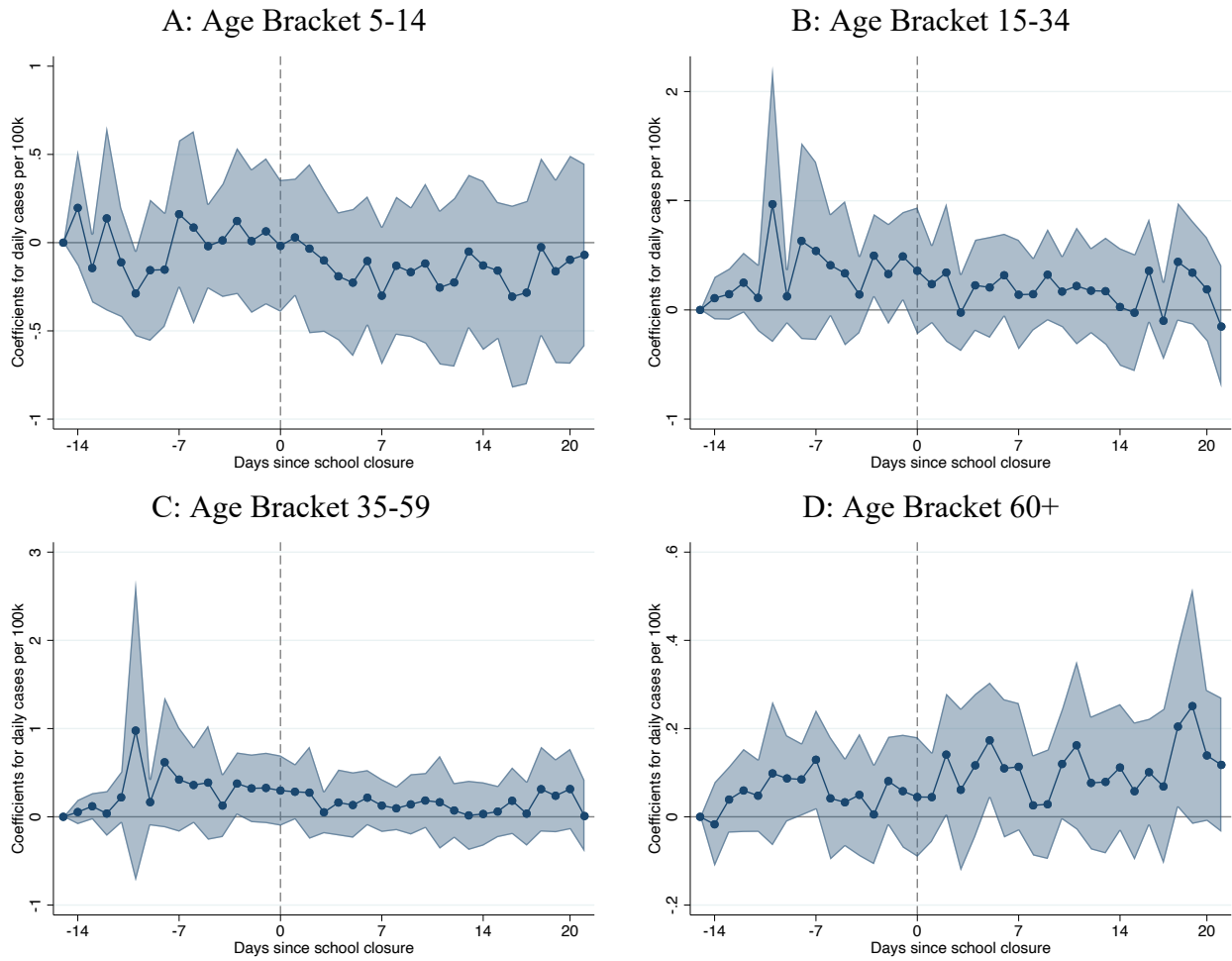
A: Age Bracket 5-14

B: Age Bracket 15-34

C: Age Bracket 35-59
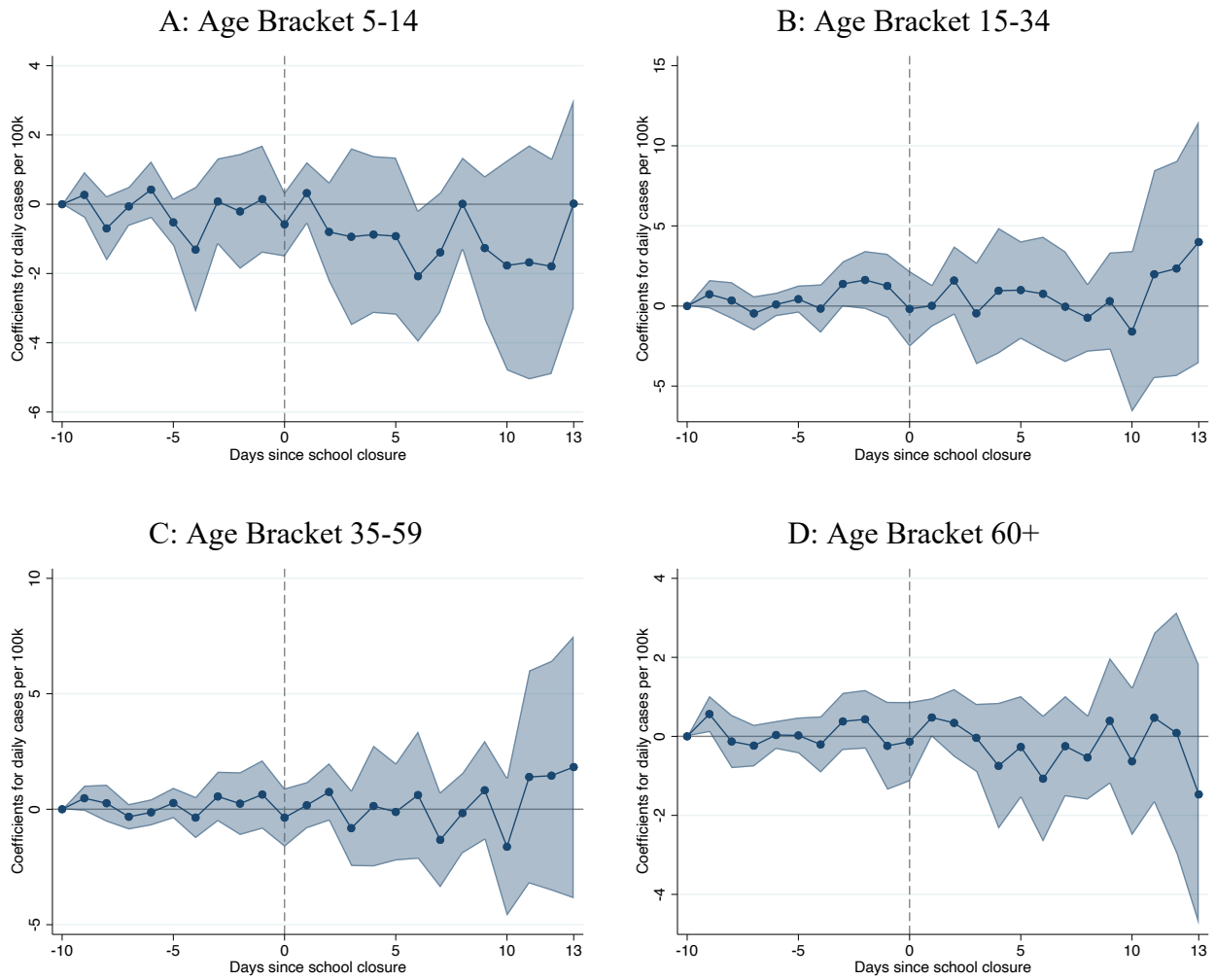
D: Age Bracket 60+

Note: The four panels, corresponding to different age brackets, display the estimates from the conventional event study specification (4) estimated by OLS with district and day fixed effects. We assume zero effects 15 or more days prior to the school closure event and drop the observations 21 and more days after the event. The regressions are weighted by the age bracket-specific local population. The shadows reflect the range inside the 95% coefficient interval, with standard errors clustered at the NUTS-2 level (38 clusters).

Figure B2: Summer School Reopening – Estimates from Conventional Event Study

A: Age Bracket 5-14

B: Age Bracket 15-34

C: Age Bracket 35-59

D: Age Bracket 60+

Note: The four panels, corresponding to different age brackets, display the estimates from the conventional event study specification (4) estimated by OLS with district and day fixed effects. We assume zero effects 15 or more days prior to the school reopening event and drop the observations 21 and more days after the event. The regressions are weighted by the age bracket-specific local population. The shadows reflect the range inside the 95% coefficient interval, with standard errors clustered at the NUTS-2 level (38 clusters).

Figure B3: Fall School Closures –Estimates from Conventional Event Study

A: Age Bracket 5-14

B: Age Bracket 15-34

C: Age Bracket 35-59

D: Age Bracket 60+

Note: The four panels, corresponding to different age brackets, display the estimates from the conventional event study specification (4) estimated by OLS with district and day fixed effects. The sample includes observations from 7 days after schools reopen after the summer holiday until the fall holiday end; we exclude all districts in Bavaria. We assume zero effects 10 or more days prior to the fall school closure event and drop the observations 14 and more days after the event. The regressions are weighted by the age bracket-specific local population. The shadows reflect the range inside the 95% coefficient interval, with standard errors clustered at the NUTS-2 level (38 clusters).
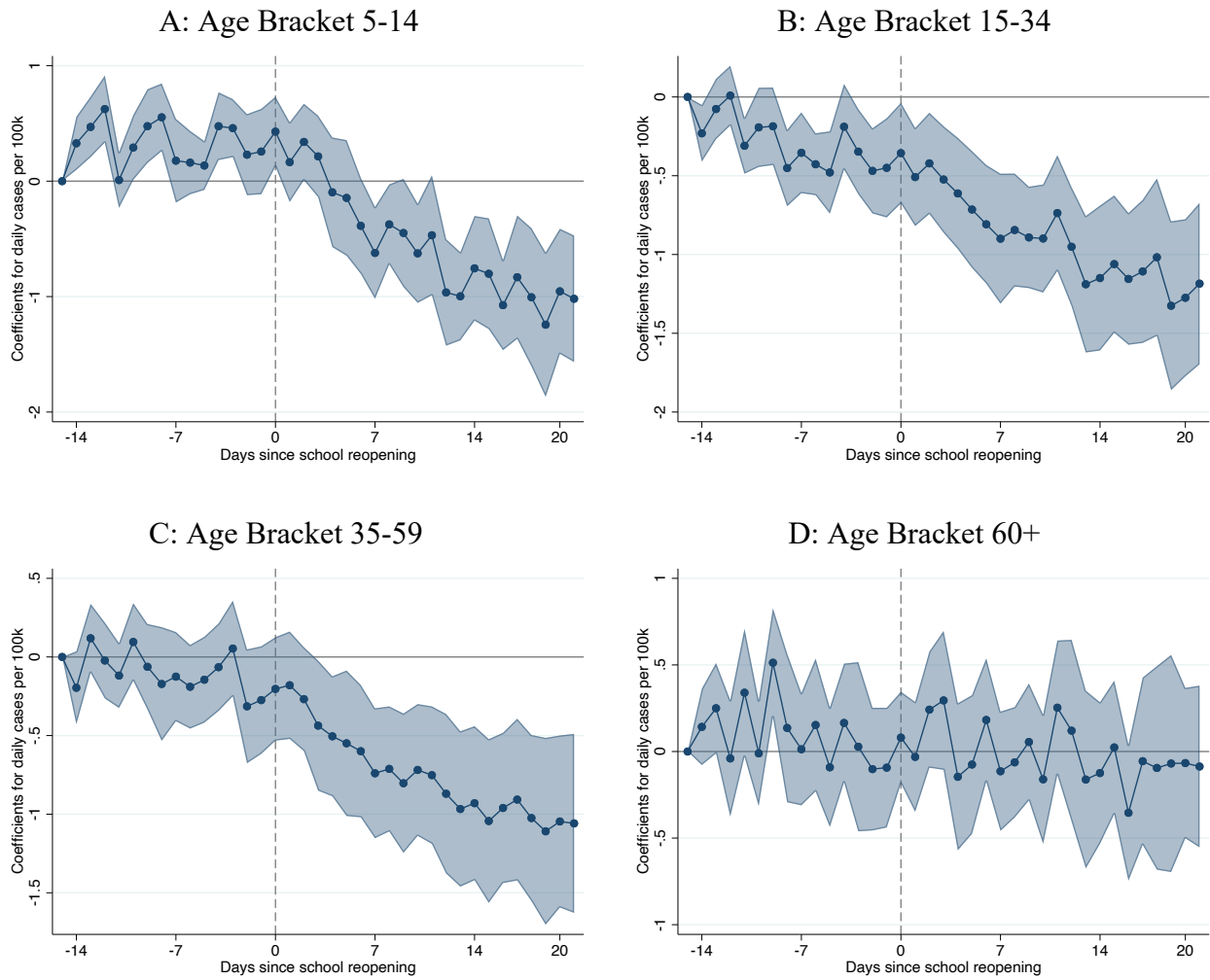
C. Estimates from Poisson Pseudo-Maximum Likelihood

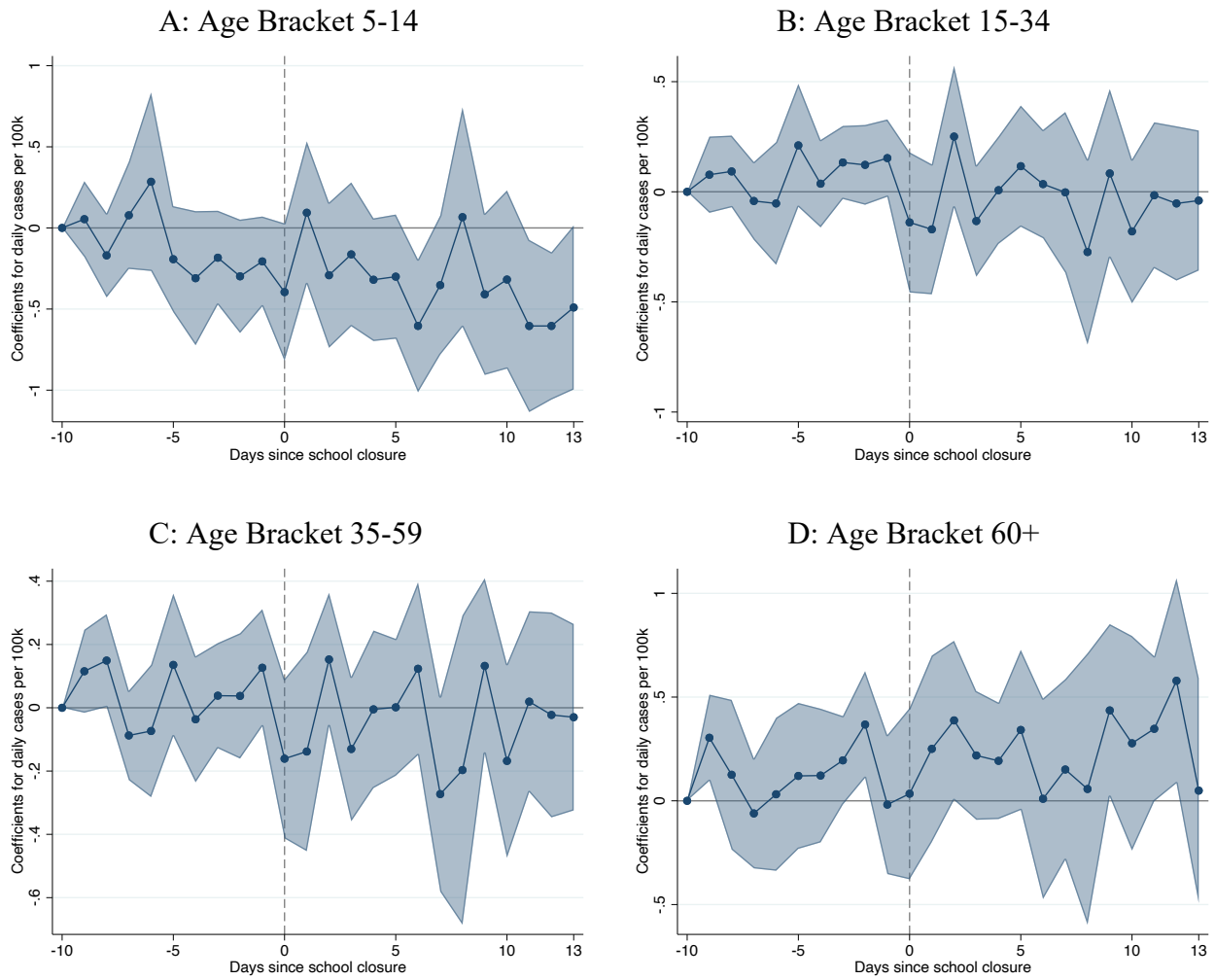Figure C1: Summer School Closures - Estimates from Poisson Pseudo-Maximum Likelihood
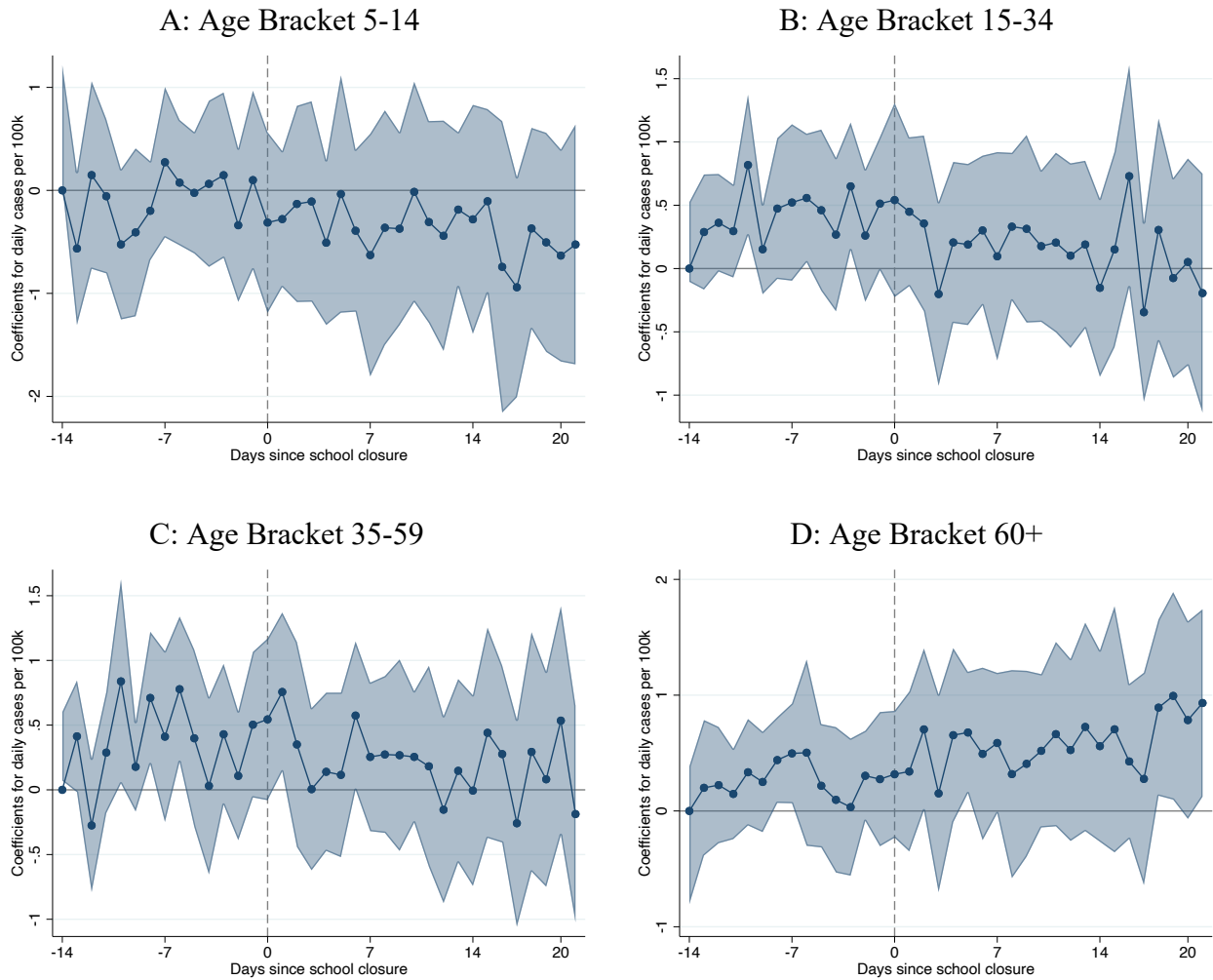
Note: The four panels, corresponding to different age brackets, display the estimates from the Poisson pseudo-maximum likelihood specification described by (5), with district and day fixed effects. We assume zero effects 15 or more days prior to the school closure event and drop the observations 21 and more days after the event. The regressions are weighted by the age bracket-specific local population. The shadows reflect the range inside the 95% coefficient interval, with standard errors clustered at the NUTS-2 level (38 clusters).

Figure C2: Summer School Reopenings - Estimates from Poisson Pseudo-Maximum Likelihood

Note: The four panels, corresponding to different age brackets, display the estimates from the Poisson pseudo-maximum likelihood specification described by (5), with district and day fixed effects. We assume zero effects 15 or more days prior to the school reopening event and drop the observations 21 and more days after the event. The regressions are weighted by the age bracket-specific local population. The shadows reflect the range inside the 95% coefficient interval, with standard errors clustered at the NUTS-2 level (38 clusters).

Figure C3: Fall School Closures - Estimates from Poisson Pseudo-Maximum Likelihood

A: Age Bracket 5-14

B: Age Bracket 15-34

C: Age Bracket 35-59

D: Age Bracket 60+

Note: The four panels, corresponding to different age brackets, display the estimates from the Poisson pseudo-maximum likelihood specification described by (5), with district and day fixed effects. The sample includes observations from 7 days after schools reopen after the fall holiday until the fall holiday end; we exclude all districts in Bavaria. We assume zero effects 10 or more days prior to the school closure event and drop the observations 14 and more days after the event. The regressions are weighted by the age bracket-specific local population. The shadows reflect the range inside the 95% coefficient interval, with standard errors clustered at the NUTS-2 level (38 clusters).
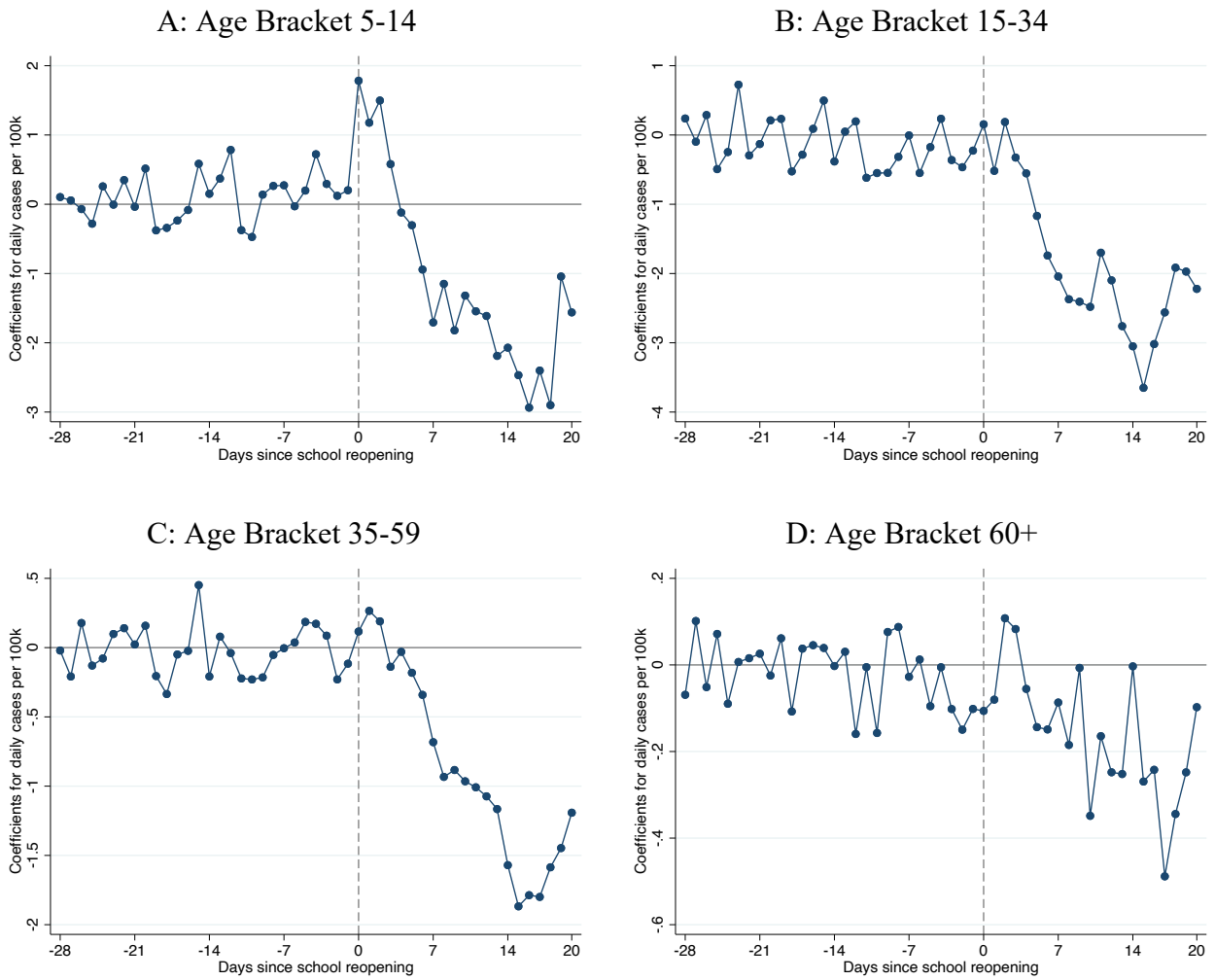
D. Estimates Using the de Chaisemartin and D'Haultfœuille (2020) Method

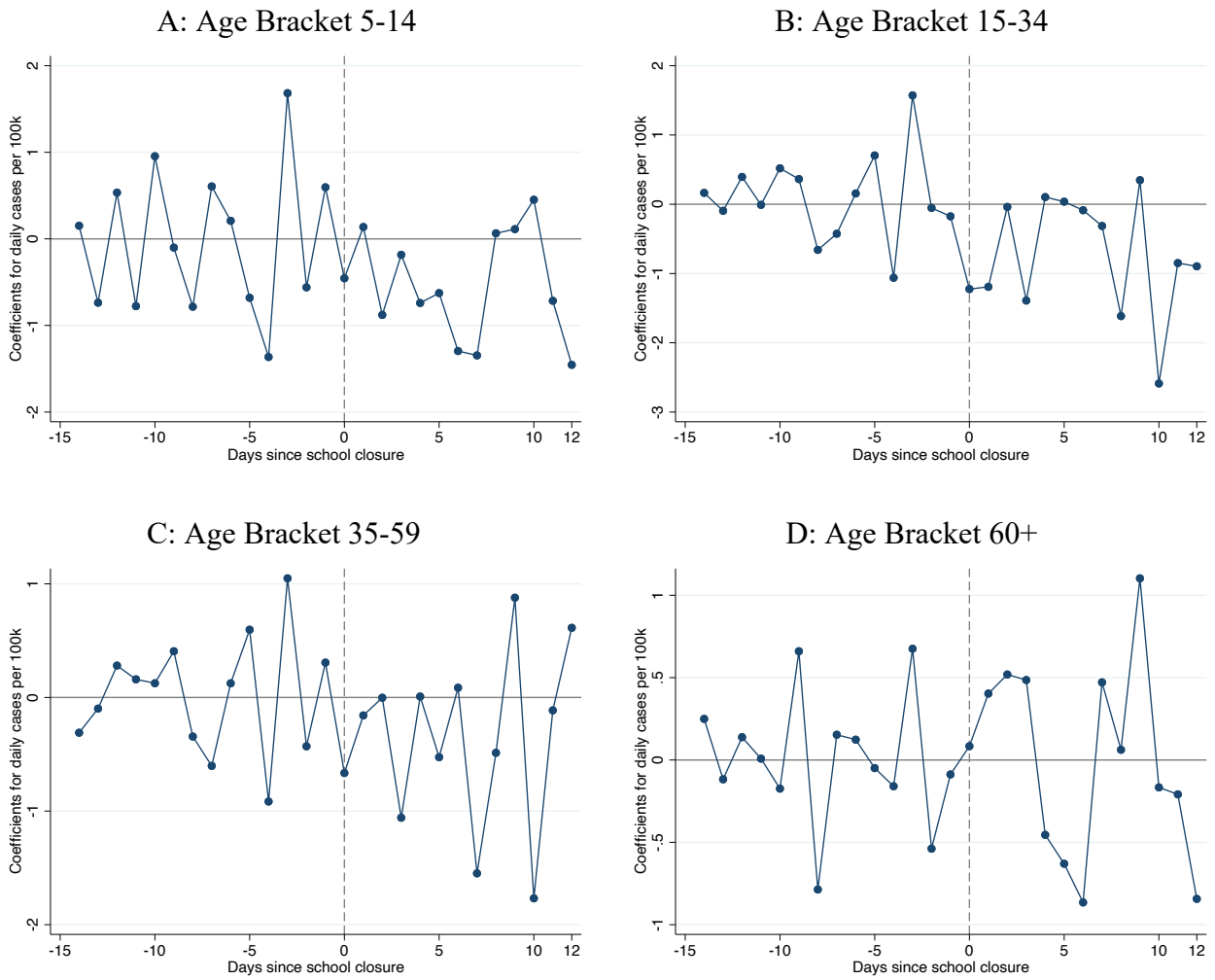Figure D1: Summer School Closures – Estimates from de Chaisemartin, D'Haultfœuille (2020)
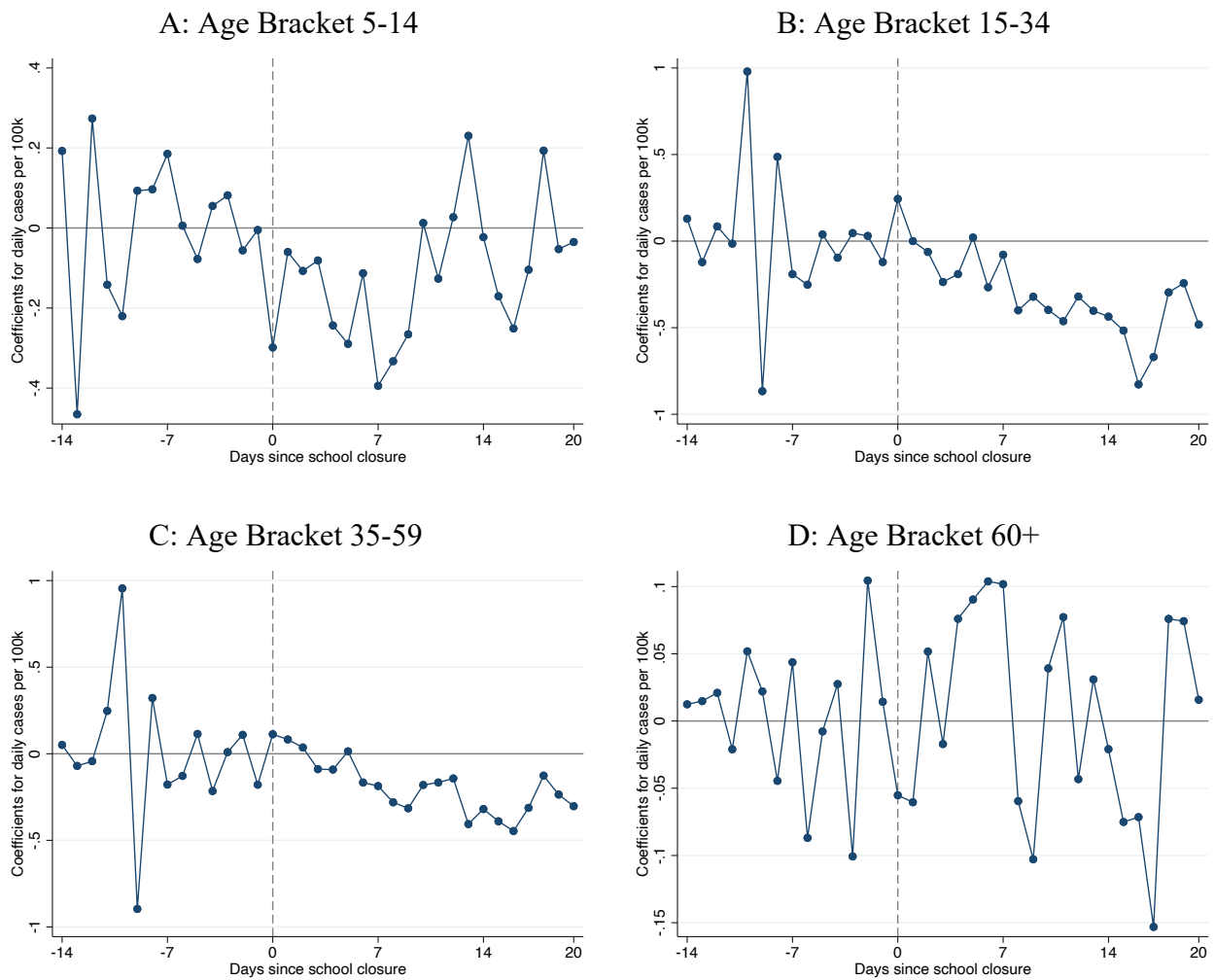
Note: The four panels, corresponding to different age brackets, display the coefficient estimates from the robust estimator developed by de Chaisemartin and D'Haultfœuille (2020) described in Section 4.4, with district and day fixed effects. The outcome variable is defined as the number of daily reported COVID-19 cases (per 100,000 in the respective age bracket), and the districts are weighted according to the age-bracket specific population.

Figure D2: Summary School Reopenings – Estimates from de Chaisemartin, D'Haultfœuille (2020)

A: Age Bracket 5-14

B: Age Bracket 15-34

C: Age Bracket 35-59

D: Age Bracket 60+

Note: The four panels, corresponding to different age brackets, display the coefficient estimates from the robust estimator developed by de Chaisemartin and D'Haultfœuille (2020) described in Section 4.4, with district and day fixed effects. We allow for anticipation effects within 14 days before schools reopened by shifting the treatment indicator 14 days forward in each state. The outcome variable is defined as the number of daily reported COVID-19 cases (per 100,000 in the respective age bracket), and the districts are weighted according to the age-bracket specific population.
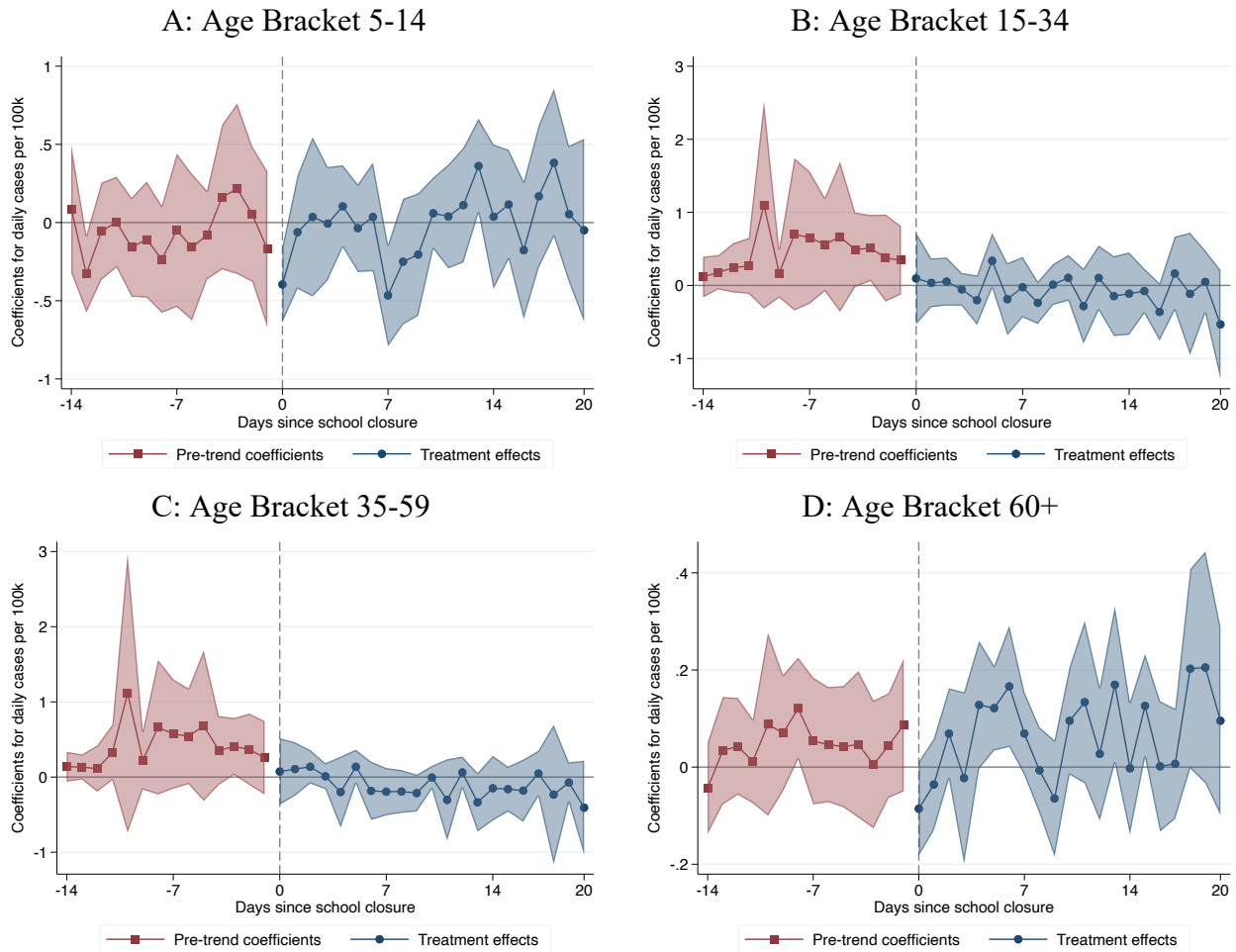
Figure D3: Fall School Closures – Estimates from de Chaisemartin, D'Haultfœuille (2020)

A: Age Bracket 5-14

B: Age Bracket 15-34

C: Age Bracket 35-59

D: Age Bracket 60+

Note: The four panels, corresponding to different age brackets, display the coefficient estimates from the robust estimator developed by de Chaisemartin and D'Haultfœuille (2020) and described in Section 4.4, including district and day fixed effects and excluding districts in Bavaria from the sample. The outcome variable is defined as the number of daily reported COVID-19 cases (per 100,000 in the respective age bracket), and the districts are weighted according to the age-bracket specific population.
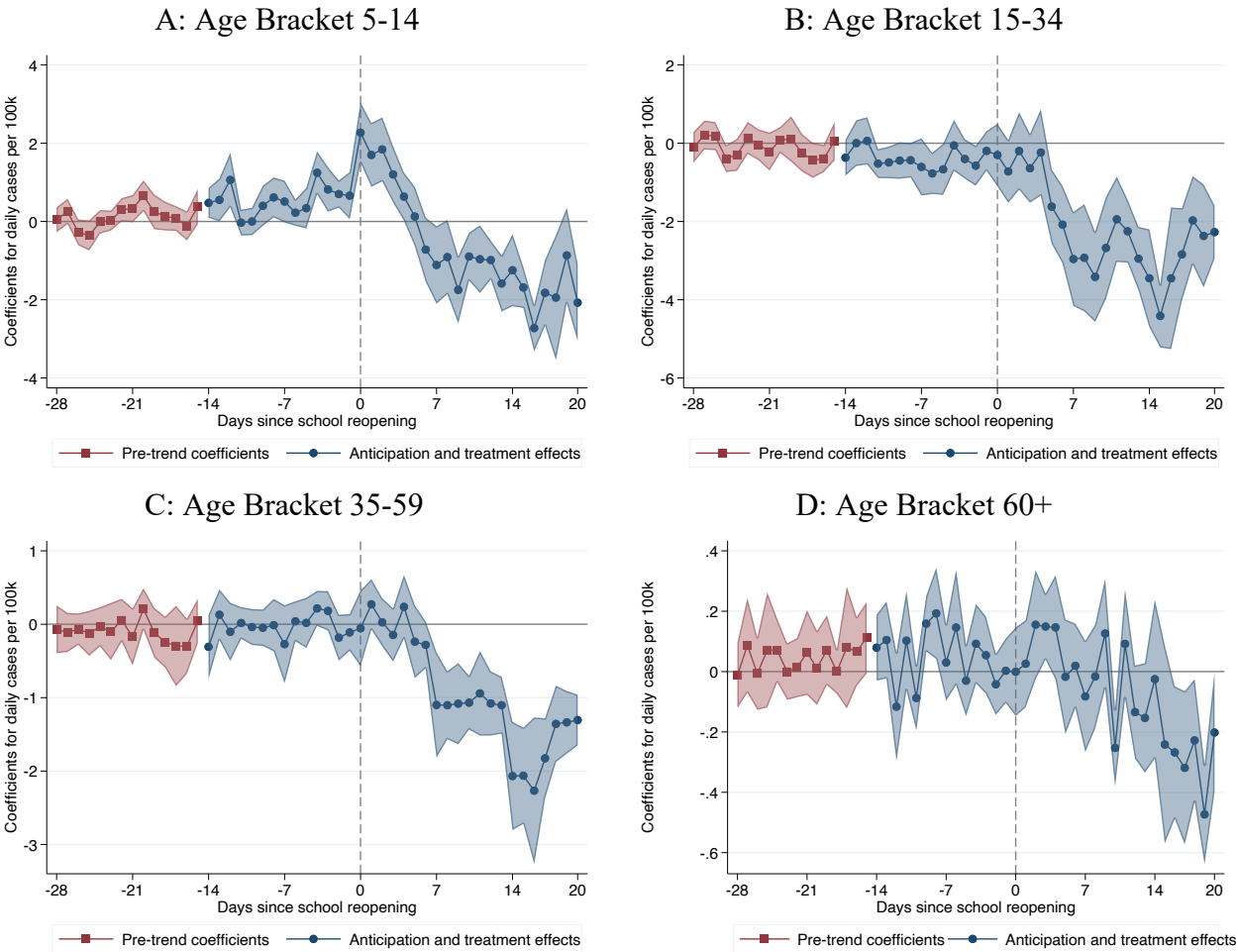
E. Including Controls

Figure E1: Summer School Closures – Estimates with Imputation Estimator and Controls
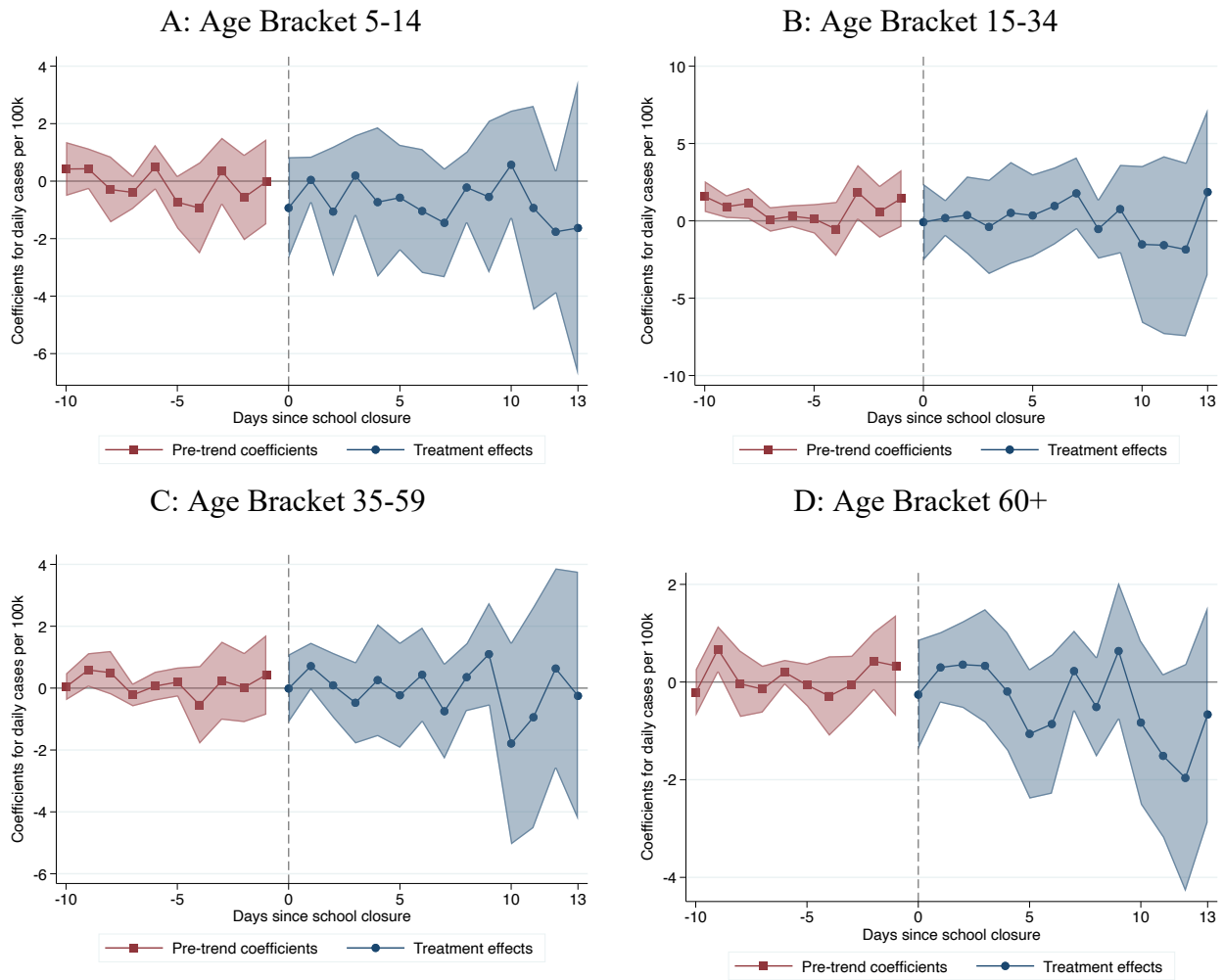

Note: The four panels, corresponding to different age brackets, display the treatment effect estimates using the Borusyak et al. (2021) imputation estimator including district and day fixed effects and a set of controls (blue dots, following equation (2)), as well as corresponding OLS estimates for pre-trends (red squares, following equation (3)). The following variables are included as controls at the imputation stage: (i) the local average daily temperature, (ii) the number of guest arrivals in accommodation facilities per capita in 2019 and exposure to a nearby international airport, both interacted with date dummies, and (iii) day of the week indicators, interacted with state fixed effects. The outcome variable is defined as the number of daily reported COVID-19 cases (per 100,000 in the respective age bracket), and the districts are weighted according to the age-bracket specific population. The shadows reflect the range inside the 95% coefficient interval, with standard errors clustered at the NUTS-2 level (38 clusters).

Figure E2: Summer School Reopenings – Estimates with Imputation Estimator with Controls

A: Age Bracket 5-14

B: Age Bracket 15-34

C: Age Bracket 35-59

D: Age Bracket 60+

Note: The four panels, corresponding to different age brackets, display the treatment effect estimates using the Borusyak et al. (2021) imputation estimator including district and day fixed effects and a set of controls (blue dots, following equation (2)), as well as corresponding OLS estimates for pre-trends (red squares, following equation (3)). The following variables are included as controls at the imputation stage: (i) the local average daily temperature, (ii) the number of guest arrivals in accommodation facilities per capita in 2019 and exposure to a nearby international airport, both interacted with date dummies, and (iii) day of the week indicators, interacted with state fixed effects. Anticipation effects are allowed within 14 days before schools reopen. The outcome variable is defined as the number of daily reported COVID-19 cases (per 100,000 in the respective age bracket), and the districts are weighted according to the age-bracket specific population. The shadows reflect the range inside the 95% coefficient interval, with standard errors clustered at the NUTS-2 level (38 clusters).
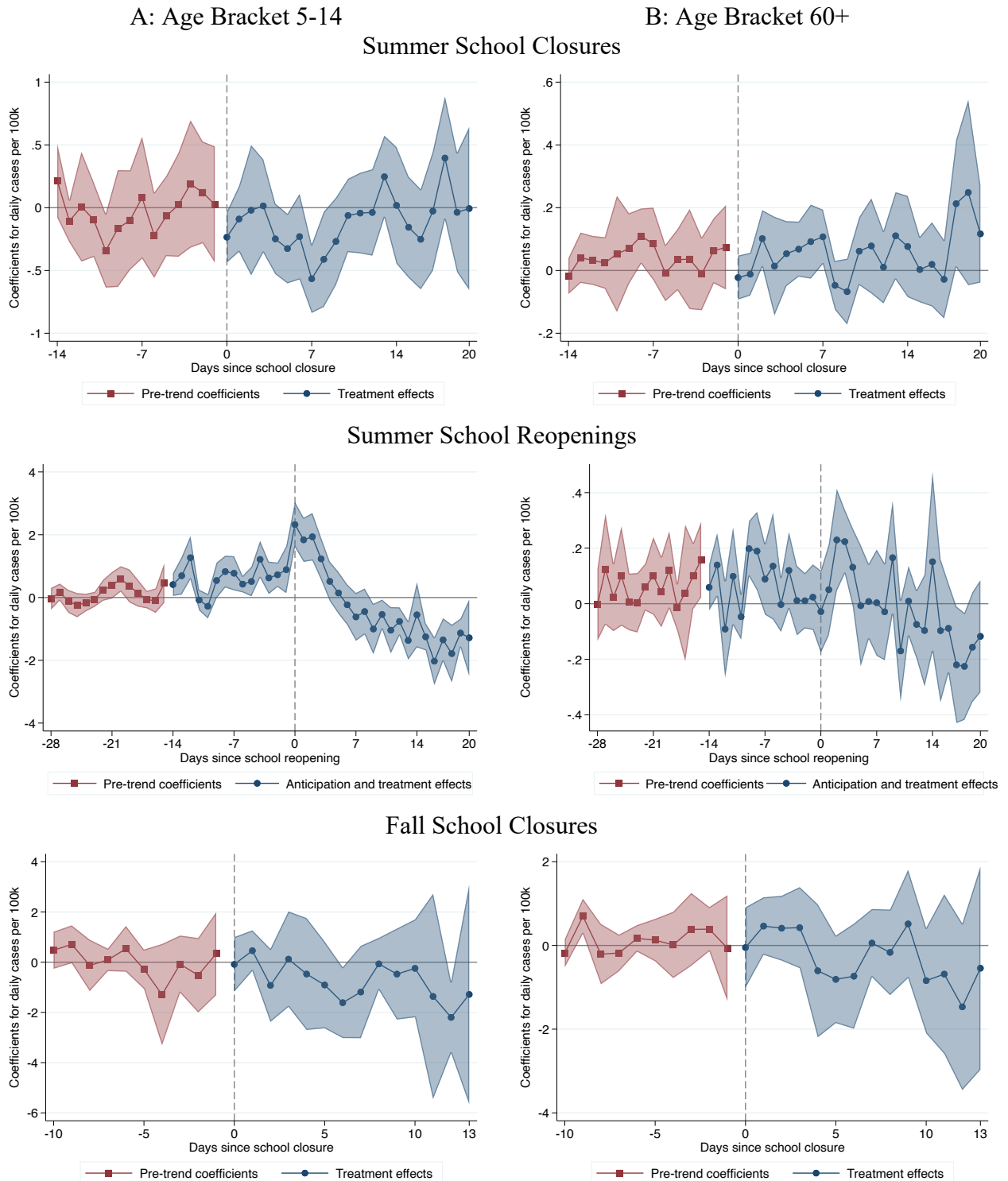
Figure E3: Fall School Closures – Estimates with Imputation Estimator with Controls

A: Age Bracket 5-14

B: Age Bracket 15-34

C: Age Bracket 35-59

D: Age Bracket 60+

Note: The four panels, corresponding to different age brackets, display the treatment effect estimates using the Borusyak et al. (2021) imputation estimator including district and day fixed effects and a set of controls (blue dots, following equation (2)), as well as corresponding OLS estimates for pre-trends (red squares, following equation (3)). The following variables are included as controls at the imputation stage: (i) the local average daily temperature, (ii) the number of guest arrivals in accommodation facilities per capita in 2019 and exposure to a nearby international airport, both interacted with date dummies, and (iii) day of the week indicators, interacted with state fixed effects. The outcome variable is defined as the number of daily reported COVID-19 cases (per 100,000 in the respective age bracket), and the districts are weighted according to the age-bracket specific population. The shadows reflect the range inside the 95% coefficient interval, with standard errors clustered at the NUTS-2 level (38 clusters).

F. Dropping Tourist Destinations

Figure F1: Estimates Dropping Tourist Destinations from the Sample

A: Age Bracket 5-14

B: Age Bracket 60+

Summer School Closures

Summer School Reopenings

Fall School Closures

Note: These figures, corresponding to the different events of interest and age brackets, repeat the analysis from Figures 5, 6, 8, 9, 14, and 15 (Panel B in all cases) on a restricted sample, dropping the top decile of districts in terms of guests per capita in accommodation services in 2019. The specifications and samples are otherwise the same. The outcome variable is defined as the number of daily reported COVID-19 cases (per 100,000 in the respective age bracket), and the districts are weighted according to the age-bracket specific population. The shadows reflect the range inside the 95% coefficient interval, with standard errors clustered at the NUTS-2 level (38 clusters).